

# Dual Smoothing and Level Set Techniques for Variational Matrix Decomposition

**Aleksandr Aravkin**

*Department of Applied Mathematics  
University of Washington  
Seattle, WA*

SARAVKIN@UW.EDU

**Stephen Becker**

*Department of Applied Mathematics  
University of Colorado, Boulder  
Boulder, CO*

STEPHEN.BECKER@COLORADO.EDU

**Citation:** chapter in “Robust Low-Rank and Sparse Matrix Decomposition: Applications in Image and Video Processing”, T. Bouwmans, N. Aybat, E. Zahzah, eds. CRC Press, 2016.

## Abstract

We focus on the robust principal component analysis (RPCA) problem, and review a range of old and new convex formulations for the problem and its variants. We then review dual smoothing and level set techniques in convex optimization, present several novel theoretical results, and apply the techniques on the RPCA problem. In the final sections, we show a range of numerical experiments for simulated and real-world problems.

## 1. Introduction

Linear superposition is a useful model for many applications, including nonlinear mixing problems. Surprisingly, we can perfectly distinguish multiple elements in a given signal using convex optimization as long as they are concise and look sufficiently different from one another. Robust principal component analysis (RPCA) is a key example, where we decompose a signal into the sum of low rank and sparse components. RPCA is a special case of *stable principal component pursuit (SPCP)*, where we also allow an explicit noise component within the RPCA decomposition. Applications include alignment of occluded images (Peng et al., 2012), scene triangulation (Zhang et al., 2011), model selection (Chandrasekaran et al., 2012), face recognition, and document indexing (Candès et al., 2011a).

For SPCP, our model is

$$A = L + S + E \tag{1}$$

where  $A$  is the observed matrix,  $L$  is a low-rank matrix,  $S$  is a sparse matrix, and  $E$  is an unstructured nuisance matrix (e.g., a stochastic error term). The classic RPCA formulation (Candès et al., 2011a) assumed  $E = 0$ , but in general we do not distinguish between RPCA and SPCP.

The RPCA problem uses regularization on the summands  $L$  and  $S$  in order to improve the recovery of the solution. In (Candès et al., 2011b), the 1-norm regularizer is applied to  $S$  to promote sparsity, and the nuclear norm is applied to  $L$  to penalize rank:

$$\min \|L\|_* + \lambda \|S\|_1 \quad \text{s.t.} \quad A = L + S. \tag{2}$$

The 1-norm  $\|\cdot\|_1$  and nuclear norm  $\|\cdot\|_*$  are given by  $\|S\|_1 = \sum_{i,j} |s_{i,j}|$  and  $\|L\|_* = \sum_i \sigma_i(L)$ , where  $\sigma(L)$  is the vector of singular values of  $L$ . The parameter  $\lambda > 0$  controls the relative importance of the low-rank term  $L$  vs. the sparse term  $S$ . This problem has been analyzed by (Chandrasekaran et al., 2009; Candès et al., 2011a), and it has perfect recovery guarantees under stylized incoherence assumptions. There is even theoretical guidance for selecting a minimax optimal regularization parameter  $\lambda$  (Candès et al., 2011a).

There are several modeling choices underlying formulation (2). First is the choice of the  $\ell_1$ -norm to promote sparsity and the trace norm (aka nuclear norm) to promote low-rank solutions. We will keep with these choices throughout the entire chapter, noting where it is possible to use more general penalties. Second, (2) assumes the data are fit exactly. Unfortunately, many practical problems only approximately satisfy the idealized assumptions. This motivates the SPCP variant:

$$\begin{aligned} \min_{L,S} \quad & \|L\|_* + \lambda_{\text{sum}} \|S\|_1 \\ \text{subject to} \quad & \|L + S - A\|_F \leq \varepsilon, \end{aligned} \tag{SPCP}_{\text{sum}}$$

where the  $\varepsilon$  parameter accounts for the unknown perturbations  $A - (L + S)$  in the data not explained by  $L$  and  $S$ . It is useful to define  $\phi(L, S) = \|L\|_* + \lambda \|S\|_1$  as a regularizer on the decision variable  $(L, S)$ . The formulation (2) then tries to find the tuple  $(\bar{L}, \bar{S})$  that fits the data perfectly, and is minimal with respect to  $\phi$ .

Third, the functional form of  $\phi$  is important; in (2) as well as (SPCP<sub>sum</sub>) the component penalties are added with a tradeoff parameter  $\lambda$ , but other choices can be made as well. In particular, Aravkin et al. (2014a) propose a new variant called ‘‘max-SPCP’’:

$$\begin{aligned} \min_{L,S} \quad & \max(\|L\|_*, \lambda_{\text{max}} \|S\|_1) \\ \text{subject to} \quad & \|L + S - A\|_F \leq \varepsilon, \end{aligned} \tag{SPCP}_{\text{max}}$$

where  $\lambda_{\text{max}} > 0$  acts similar to  $\lambda_{\text{sum}}$ , and this new formulation offers both modeling and computational advantages over (SPCP<sub>sum</sub>) (see Section 5.2). We show that cross-validation with (SPCP<sub>max</sub>) to estimate  $(\lambda_{\text{max}}, \varepsilon)$  is significantly easier than estimating  $(\lambda_{\text{sum}}, \varepsilon)$  in (SPCP<sub>sum</sub>). Given an *oracle* that provides an ideal separation  $A \simeq L_{\text{oracle}} + S_{\text{oracle}}$ , we can use  $\varepsilon = \|L_{\text{oracle}} + S_{\text{oracle}} - A\|_F$  in both cases. However, while we can estimate  $\lambda_{\text{max}} = \|L_{\text{oracle}}\|_* / \|S_{\text{oracle}}\|_1$ , it is not clear how to choose  $\lambda_{\text{sum}}$  from data, without using cross-validation or assuming a probabilistic model.

Finally, both (SPCP<sub>sum</sub>) and (SPCP<sub>max</sub>) assume a least-squares penalty functional to measure the error up to level  $\varepsilon$ . We can consider a more general choice of penalty  $\rho$ :

$$\min \phi(L, S) \quad \text{s.t.} \quad \rho(A - L - S) \leq \varepsilon. \tag{3}$$

Robust losses as well as  $\rho$  arising from probabilistic models have been explored in (Aravkin et al., 2014c, 2016).

Once  $\rho$  and  $\phi$  have been selected, we can choose the type of regularization formulation one wants to solve. Formulation (3) minimizes the regularizer subject to a constraint on the misfit error. Two other common formulations are

$$\min \rho(A - L - S) \quad \text{s.t.} \quad \phi(L, S) \leq \tau, \tag{4}$$

which minimizes the error subject to a constraint on the regularizer, and

$$\min \rho(A - L - S) + \lambda \phi(L, S), \tag{5}$$

which minimizes the sum of error and regularizer with another tradeoff parameter to balance these goals.

All three formulations can be effectively used, and are equivalent in the sense that solutions match for certain values of parameters  $\lambda$ ,  $\tau$ , and  $\varepsilon$ . Formulation (3) is preferable from a modeling perspective when the misfit level  $\varepsilon$  is known ahead of time, or can be estimated. However, formulations (4) and (5) often have fast first-order algorithms available for their solution.

It turns out that we can exploit algorithms for (4) to solve (3) using the graph of the value function for problem (4); this relationship can be used to show that the problems have the same complexity (Aravkin et al., 2016). Level set optimization was first applied for sparsity optimization by van den Berg and Friedlander (2008), and later extended to gauge optimization (van den Berg and Friedlander, 2011) and to general convex programming (Aravkin et al., 2013).

The second approach we consider is the TFOCS algorithm (Becker et al., 2011) and software<sup>1</sup>, which is based on the proximal point algorithm, and can also handle generic convex minimization problems. We present a new analysis of TFOCS, along with stronger convergence guarantees, and also apply TFOCS method to RPCA. TFOCS solves all standard variants of RPCA and SPCP, and can easily add non-negativity or other types of additional constraints. We briefly detail how the algorithm can be specialized for the RPCA problem in particular.

The chapter proceeds as follows. In Section 2, we provide the necessary convex analysis background to understand our algorithms and results. In Section 3, we look at level set techniques in the context of the RPCA problem; in particular we describe previous work and algorithms for SPCP and RPCA in Section 3.2, discuss computationally efficient projections as optimization workhorses in Section 3.4, and develop new accelerated projected quasi-Newton methods for the flipped and Lagrangian formulations in Section 3.5. We then present a view of dual smoothing, describe the TFOCS algorithm, and show to to apply it to RPCA in Section 4. We describe the general class of problems solvable by TFOCS in Section 4.1, detail the dual smoothing approach in Section 4.2, and present new convergence results in Section 4.5. Finally, we demonstrate the efficacy of the new solvers and the overall formulation on synthetic problems and real data problems in Section 5.

## 2. Convex Analysis Background

We work in finite dimensional spaces  $\mathbb{R}^n$  (with Euclidean inner product) unless otherwise specified; we note however that much of the general theory below generalizes immediately to Hilbert spaces and some of it to Banach spaces. Standard definitions are not referenced, but can be found in convex analysis textbooks (Rockafellar, 1970b; Rockafellar and Wets, 1998) or in review papers such as Combettes and Pesquet (2011).

### 2.1 Key definitions

In this section, we provide definitions of objects that we use throughout the chapter.

We work with functions that take on values from the extended real line  $\overline{\mathbb{R}} := \mathbb{R} \cup \{\infty\}$ . For example, we define the indicator function as follows:

---

1. <http://cvxr.com/tfocs>

**Definition 1 (Indicator Function of a set  $C$ )**

$$\chi_C(x) = \begin{cases} 0 & x \in C \\ +\infty & x \notin C \end{cases}$$

and thus for any functional  $f$  on  $\mathbb{R}^n$ ,

$$\min_{x \in C} f(x) = \min_{x \in \mathbb{R}^n} f(x) + \chi_C(x).$$

This allows a unified treatment of constraints and objectives by encoding constraints using indicator functions.

The class  $\Gamma_0(\mathbb{R}^n)$  denotes **convex, lower semi-continuous (lsc), proper** functionals from  $\mathbb{R}^n$  to  $\overline{\mathbb{R}}$ . A function is lsc if and only if its graph is closed, and in particular a continuous function is lsc. A proper function is not identically equal to  $+\infty$  and is never  $-\infty$ . We write  $\text{dom } f = \{x \mid f(x) < \infty\}$ . Further background is widely available, e.g., (Rockafellar, 1970b; Combettes and Pesquet, 2011).

**Definition 2 (Subdifferential and subgradient)** *Let  $f \in \Gamma_0(\mathbb{R}^n)$ , then the **subdifferential** of  $f$  at the point  $x \in \text{dom } f$  is the set*

$$\partial f(x) = \{d \in \mathbb{R}^n \mid \forall y \in \mathbb{R}^n, f(y) \geq f(x) + \langle d, y - x \rangle\}$$

and elements of the set are known as **subgradients**.

The sub-differential of an indicator function  $\chi_C$  at  $x$  is the normal cone to  $C$  at  $x$ . Fermat's rule is that  $x \in \arg \min f(x)$  iff  $0 \in \partial f(x)$ , which follows by the definition of the subdifferential. If  $f, g \in \Gamma_0(\mathbb{R}^n)$ , then  $\partial(f+g) = \partial f + \partial g$  in many situations (i.e., under constraint qualifications such as  $f$  or  $g$  having full domain). In finite dimensions, Gâteaux and Fréchet differentiability coincide on  $\Gamma_0(\mathbb{R}^n)$  and  $\partial f(x) = \{d\}$  iff  $f$  is differentiable at  $x$  with  $\nabla f(x) = d$ .

We now introduce a key generalization of projections that will be used widely.

**Definition 3 (Proximity operator)** *If  $f \in \Gamma_0(\mathbb{R}^n)$  and  $\lambda > 0$ , define*

$$\text{Prox}_{\lambda f}(y) = \arg \min_x \lambda f(x) + \frac{1}{2} \|x - y\|^2 = (I + \lambda \partial f)^{-1}(y)$$

Note that even though  $\partial f$  is potentially multi-valued, the proximity operator is always uniquely defined (if  $f \in \Gamma_0(\mathbb{R}^n)$ ), since it is the minimizer of a strongly convex function. When we say that a proximity operator for  $f$  is easy to compute, we mean that the proximity operator for  $\lambda f$  is easy to compute for all  $\lambda > 0$ . Computational complexity will be explored in more detail in subsequent sections.

The proximity operator generalizes projection, since  $\text{Prox}_{\chi_C}(y) = \text{Proj}_C(y)$  where  $\text{Proj}$  denotes orthogonal projection onto a set. Another example is the proximity operator of the  $\ell^1$  norm, which is equivalent to soft-thresholding. The proximity operator is firmly non-expansive (Combettes and Pesquet, 2011), just like orthogonal projections.

**Definition 4 ((Fenchel-Legendre) Conjugate function)** *Let  $f \in \Gamma_0(\mathbb{R}^n)$ , then the **conjugate function**  $f^*$  is defined*

$$f^*(y) = \sup_x \langle x, y \rangle - f(x).$$

Furthermore,  $\partial f^* = (\partial f)^{-1}$ , where  $(\cdot)^{-1}$  is the pre-image operation, and  $f^{**} = f$ .

**Definition 5 (Gauge)** For a convex set  $C$  containing the origin, the gauge  $\gamma(x | C)$  is defined by

$$\gamma(x | C) = \inf_{\lambda} \{\lambda : x \in \lambda C\}. \quad (6)$$

For any norm  $\|\cdot\|$ , the set defining it as a gauge is simply the unit ball  $\mathbb{B}_{\|\cdot\|} = \{x : \|x\| \leq 1\}$ . Gauges are useful in our computational context since they easily allow some extensions, such as inclusion of non-negativity constraints.

We make extensive use of the theory of dual functions. For example, if one can compute  $\text{Prox}_f$ , then one can compute  $\text{Prox}_{f^*}$  and related quantities as well, using

$$\text{Prox}_{f^*}(x) = x - \text{Prox}_f(x) \quad (7)$$

$$\text{Prox}_{\check{f}}(x) = -\text{Prox}_f(-x) \quad (8)$$

where  $\check{f}(x) = f(-x)$ .

**Definition 6 (Relative interior)** The *relative interior* (ri) of a set  $C \subset \mathbb{R}^n$  is the interior of  $C$  relative to its affine hull (the smallest affine space containing  $C$ ).

**Definition 7 (Lipschitz continuity)** A function  $F : \mathbb{R}^n \rightarrow \mathbb{R}^m$  is Lipschitz continuous with constant  $\ell$  if  $\ell$  is the smallest real number such that for all  $x, x' \in \mathbb{R}^n$ ,

$$\|F(x) - F(x')\|_{\mathbb{R}^m} \leq \ell \|x - x'\|_{\mathbb{R}^n}.$$

### 3. Level-set methods for Residual-Constrained SPCP

In this section, we discuss a range of convex formulations for SPCP, their relationships, and survey prior art. We then show how to apply level set methods to several of the formulations.

#### 3.1 A primer on SPCP

We illustrate  $(\text{SPCP}_{\text{sum}})$  and  $(\text{SPCP}_{\text{max}})$  via different convex formulations. Flipping the objective and the constraints in  $(\text{SPCP}_{\text{max}})$  and  $(\text{SPCP}_{\text{sum}})$ , we obtain the following convex programs

$$\begin{aligned} \min_{L, S} \quad & \rho(L + S - A) \\ \text{s.t.} \quad & \| \|L\|_* + \lambda_{\text{sum}} \|S\|_1 \leq \tau_{\text{sum}} \end{aligned} \quad (\text{flip-SPCP}_{\text{sum}})$$

$$\begin{aligned} \min_{L, S} \quad & \rho(L + S - A) \\ \text{s.t.} \quad & \max(\| \|L\|_*, \lambda_{\text{max}} \|S\|_1) \leq \tau_{\text{max}} \end{aligned} \quad (\text{flip-SPCP}_{\text{max}})$$

Solutions of  $(\text{flip-SPCP}_{\text{sum}})$  and  $(\text{flip-SPCP}_{\text{max}})$  are implicitly related to the solutions of  $(\text{SPCP}_{\text{sum}})$  and  $(\text{SPCP}_{\text{max}})$  via the Pareto frontier by Aravkin et al. (2013, Theorem 2.1). While in many applications,  $\rho(\cdot)$  is taken to be the 2-norm squared, the relationship holds in general. For the range of parameters where the constraints in  $(\text{SPCP}_{\text{sum}})$  and  $(\text{SPCP}_{\text{max}})$  are *active*, for any parameter  $\varepsilon$  there exist corresponding parameters  $\tau_{\text{sum}}(\varepsilon)$  and  $\tau_{\text{max}}(\varepsilon)$ , for which the optimal value of  $(\text{flip-SPCP}_{\text{sum}})$  and  $(\text{flip-SPCP}_{\text{max}})$  is  $\varepsilon$ , and the corresponding optimal solutions  $(\bar{S}_s, \bar{L}_s)$  and  $(\bar{S}_m, \bar{L}_m)$  are also optimal for  $(\text{SPCP}_{\text{sum}})$  and  $(\text{SPCP}_{\text{max}})$ .

For completeness, we also include the Lagrangian formulation:

$$\min_{L,S} \lambda_L \|L\|_* + \lambda_S \|S\|_1 + \frac{1}{2} \|L + S - A\|_F^2 \quad (\text{lag-SPCP})$$

Problems (**flip-SPCP<sub>max</sub>**) and (**flip-SPCP<sub>sum</sub>**) can be solved using projected gradient optimal projected gradient methods. The disadvantage of some of these formulations is that it is again not as clear how to tune the parameters. We show that one can solve (**SPCP<sub>max</sub>**) and (**SPCP<sub>sum</sub>**) using a sequence of flipped problems; moreover this approach inherits the computational complexity guarantees of (**flip-SPCP<sub>max</sub>**) and (**flip-SPCP<sub>sum</sub>**) (Aravkin et al., 2016). In practice, better tuning also leads to faster algorithms, e.g., fixing  $\varepsilon$  ahead of time to an estimated ‘noise floor’ greatly reduces the amount of required computation if parameters are to be selected via cross-validation.

Finally, in some cases, it is useful to change the  $\rho(L + S - A)$  term to  $\rho(\mathcal{L}(L + S - A))$  where  $\mathcal{L}$  is a linear operator. For example, let  $\Omega$  be a subset of the indices of a  $m \times n$  matrix. We may only observe  $A$  restricted to these entries, denoted  $\text{Proj}_\Omega(A)$ , in which case we choose  $\mathcal{L} = \text{Proj}_\Omega$ . Most existing RPCA/SPCP algorithms adapt to the case  $\mathcal{L} = \text{Proj}_\Omega$  but this is due to the strong properties of the projection operator  $\text{Proj}_\Omega$ . The advantage of our approach is that it seamlessly handles arbitrary linear operators  $\mathcal{L}$ .

### 3.2 Prior Art

While problem (**SPCP<sub>sum</sub>**) with  $\varepsilon = 0$  has several solvers (e.g., it can be solved by applying the widely known Alternating Directions Method of Multipliers (ADMM)/ Douglas-Rachford method (Combettes and Pesquet, 2007)), the formulation assumes the data are noise free. Unfortunately, the presence of noise we consider in this paper introduces a third term in the ADMM framework, where extra care must be taken to develop a convergent variant of ADMM (Chen et al., 2013). Interestingly, there are only a handful of methods that can handle this case. Those using smoothing techniques no longer promote exactly sparse and/or exactly low-rank solutions. Those using dual decomposition techniques may require high iteration counts. Because each step requires a partial singular value decomposition (SVD) of a large matrix, it is critical that the methods only take a few iterations.

As a rough comparison, we start with related solvers that solve (**SPCP<sub>sum</sub>**) for  $\varepsilon = 0$ . Wright et al. (2009a) solves an instance of (**SPCP<sub>sum</sub>**) with  $\varepsilon = 0$  and a  $800 \times 800$  system in 8 hours. By switching to the (**lag-SPCP**) formulation, Ganesh et al. (2009) uses the accelerated proximal gradient method (Beck and Teboulle, 2009a) to solve a  $1000 \times 1000$  matrix in under one hour. This is improved further in Lin et al. (2010) which again solves (**SPCP<sub>sum</sub>**) with  $\varepsilon = 0$  using the augmented Lagrangian and ADMM methods and solves a  $1500 \times 1500$  system in about a minute. As a prelude to our results, our method can solve some systems of this size in about 10 seconds (c.f., Fig. 4).

In the case of (**SPCP<sub>sum</sub>**) with  $\varepsilon > 0$ , Tao and Yuan (2011) propose the alternating splitting augmented Lagrangian method (ASALM), which exploits separability of the objective in the splitting scheme, and can solve a  $1500 \times 1500$  system in about five minutes.

The partially smooth proximal gradient (PSPG) approach of Aybat et al. (2013) smooths just the nuclear norm term and then applies the well-known FISTA algorithm (Beck and Teboulle, 2009a). Aybat et al. (2013) show that the proximity step can be solved efficiently in closed-form, and the dominant cost at every iteration is that of the partial SVD. They include some examples on video, solving  $1500 \times 1500$  formulations in under half a minute.

The nonsmooth adaptive Lagrangian (NSA) algorithm of Aybat and Iyengar (2013) is a variant of the ADMM for (**SPCP<sub>sum</sub>**), and makes use of the insight of Aybat et al. (2013). The ADMM variant

is interesting in that it splits the variable  $L$ , rather than the sum  $L + S$  or residual  $L + S - A$ . Their experiments solve a  $1500 \times 1500$  synthetic problems in between 16 and 50 seconds (depending on accuracy).

Shen et al. (2014) develops a method exploiting low-rank matrix factorization scheme, maintaining  $L = UV^T$ . This technique has also been effectively used in practice for matrix completion (Lee et al., 2010; Aravkin et al., 2014b), but lacks a full convergence theory in either context. The method of Shen et al. (2014) was an order of magnitude faster than ASALM, but encountered difficulties in some experiments where the sparse component dominated the low rank component. We note that the factorization technique may potentially speed up some of the methods presented here, but we leave this to future work, and only work with convex formulations.

### 3.3 Level set methods for Sum-SPCP and Max-SPCP

Recall that both (SPCP<sub>sum</sub>) and (SPCP<sub>max</sub>) can be written as follows:

$$\min \phi(L, S) \quad \text{s.t.} \quad \rho(L + S - A) \leq \varepsilon. \quad (9)$$

Earlier, we discussed that both  $\phi$  and  $\rho$  can be chosen by the modeler; in particular sum and max formulations come from choosing  $\phi_{\text{sum}}$  vs.  $\phi_{\text{max}}$ . While classic formulations assume  $\rho$  to be the Frobenius norm, this restriction is not necessary, and we consider  $\rho$  to be smooth and convex. In particular,  $\rho$  can be taken to be the robust Huber penalty (Huber, 2004). Even more importantly, this formulation allows pre-composition of a smooth convex penalty with an arbitrary linear operator  $\mathcal{L}$ . In particular, note that the RPCA model is described by a simple linear operator:

$$L + S = \begin{bmatrix} I & I \end{bmatrix} \begin{bmatrix} L \\ S \end{bmatrix}. \quad (10)$$

Projection onto a set of observed indices  $\Omega$  is also a simple linear operator that can be included in  $\rho$ . Operators may include different transforms (e.g., Fourier) applied to either  $L$  or  $S$ .

The problem class (9) falls into the class of problems studied by van den Berg and Friedlander (2011, 2008) for  $\rho(\cdot) = \|\cdot\|^2$  and by Aravkin et al. (2013) for arbitrary convex  $\rho$ . Following these references, we define the *value function*  $v(\tau)$  as

$$v(\tau) = \min_{L, S} \rho(\mathcal{L}(L, S) - A) \quad \text{s.t.} \quad \phi(L, S) \leq \tau. \quad (11)$$

This value function provides the bridge between formulations of type (9) and their ‘flipped’ counterparts. Specifically, one can use Newton’s method to find a solution to  $v(\tau) = \varepsilon$ . The approach is agnostic to the linear operator  $\mathcal{L}$  (it can be of the simple form (10), or include restriction in the missing data case, etc.).

For both formulations of interest,  $\phi$  is a norm defined on a product space  $\mathbb{R}^{n \times m} \times \mathbb{R}^{n \times m}$ , since we can write

$$\phi_{\text{sum}}(L, S) = \left\| \begin{bmatrix} \|L\|_* \\ \lambda_{\text{sum}} \|S\|_1 \end{bmatrix} \right\|_1, \quad (12)$$

$$\phi_{\text{max}}(L, S) = \left\| \begin{bmatrix} \|L\|_* \\ \lambda_{\text{max}} \|S\|_1 \end{bmatrix} \right\|_\infty. \quad (13)$$

In particular, both  $\phi_{\text{sum}}(L, S)$  and  $\phi_{\text{max}}(L, S)$  are gauges as well as norms, and since we are able to treat this level of generality, we focus our theoretical results on this wider class.

In order to implement Newton's method for (11), the optimization problem to evaluate  $v(\tau)$  must be solved (fully or approximately) to obtain  $(\bar{L}, \bar{S})$ . Then the  $\tau$  parameter for the next (11) problem is updated via

$$\tau^{k+1} = \tau^k - \frac{v(\tau^k) - \epsilon}{v'(\tau^k)}. \quad (14)$$

Given  $(\bar{L}, \bar{S})$ ,  $v'(\tau)$  can be written in closed form using Aravkin et al. (2013, Theorem 5.2), which simplifies to

$$v'(\tau) = -\phi^\circ(\mathcal{L}^T \nabla \rho(\mathcal{L}(\bar{L}, \bar{S}) - A)), \quad (15)$$

with  $\phi^\circ$  denoting the polar gauge to  $\phi$ . The polar gauge is precisely  $\gamma(x | C^\circ)$ , with

$$C^\circ = \{v : \langle v, x \rangle \leq 1 \quad \forall x \in C\}. \quad (16)$$

In the simplest case, where  $\mathcal{L}$  is given by (10), and  $\rho$  is the least squares penalty, the formula (15) becomes

$$v'(\tau) = -\phi^\circ \left( \begin{bmatrix} \bar{L} + \bar{S} - A \\ \bar{L} + \bar{S} - A \end{bmatrix} \right).$$

The main computational challenge in the approach outlined in (11)-(15) is to design a fast solver to evaluate  $v(\tau)$ . Section 3.5 does just this.

The key to RPCA is that the regularization functional  $\phi$  is a gauge over the product space used to decompose  $A$  into summands  $L$  and  $S$ . This makes it straightforward to compute polar results for both  $\phi_{\text{sum}}$  and  $\phi_{\text{max}}$ .

**Theorem 8 (Max-Sum Duality for Gauges on Product Spaces)** *Let  $\gamma_1$  and  $\gamma_2$  be gauges on  $\mathbb{R}^{n_1}$  and  $\mathbb{R}^{n_2}$ , and consider the function*

$$g(x, y) = \max\{\gamma_1(x), \gamma_2(y)\}.$$

*Then  $g$  is a gauge, and its polar is given by*

$$g^\circ(z_1, z_2) = \gamma_1^\circ(z_1) + \gamma_2^\circ(z_2).$$

**Proof** Let  $C_1$  and  $C_2$  denote the canonical sets corresponding to gauges  $\gamma_1$  and  $\gamma_2$ . It immediately follows that  $g$  is a gauge for the set  $C = C_1 \times C_2$ , since

$$\begin{aligned} \inf\{\lambda \geq 0 | (x, y) \in \lambda C\} &= \inf\{\lambda | x \in \lambda C_1 \text{ and } y \in \lambda C_2\} \\ &= \max\{\gamma_1(x), \gamma_2(y)\}. \end{aligned}$$

By Rockafellar (1970a, Corollary 15.1.2), the polar of the gauge of  $C$  is the support function of  $C$ , which is given by

$$\begin{aligned} \sup_{x \in C_1, y \in C_2} \langle (x, y), (z_1, z_2) \rangle &= \sup_{x \in C_1} \langle x, z_1 \rangle + \sup_{y \in C_2} \langle y, z_2 \rangle \\ &= \gamma_1^\circ(z_1) + \gamma_2^\circ(z_2). \end{aligned}$$

■

This theorem allows us to easily compute the polars for  $\phi_{\text{sum}}$  and  $\phi_{\text{max}}$  in terms of the polars of  $\|\cdot\|_*$  and  $\|\cdot\|_1$ , which are the dual norms of the spectral norm and infinity norm, respectively.

**Corollary 9 (Explicit variational formulas for (SPCP<sub>sum</sub>) and (SPCP<sub>max</sub>))** *We have*

$$\begin{aligned}\phi_{sum}^\circ(Z_1, Z_2) &= \max \left\{ \|Z_1\|_2, \frac{1}{\lambda_{sum}} \|Z_2\|_\infty \right\} \\ \phi_{max}^\circ(Z_1, Z_2) &= \|Z_1\|_2 + \frac{1}{\lambda_{max}} \|Z_2\|_\infty,\end{aligned}\tag{17}$$

where  $\|X\|_2$  denotes the spectral norm (square root of the largest eigenvalue of  $X^T X$ ) and  $\|X\|_\infty$  denotes the largest entry in absolute value.

We now have closed form solutions for  $v'(\tau)$  in (15) for both formulations of interest. The remaining challenge is to design a fast solver for (11) for formulations (SPCP<sub>sum</sub>) and (SPCP<sub>max</sub>). We focus on this challenge in the remaining sections of the paper. We also discuss the advantage of (SPCP<sub>max</sub>) from this computational perspective.

### 3.4 Projections

In this section, we consider the computational issues of projecting onto the set defined by  $\phi(L, S) \leq \tau$ . For  $\phi_{max}(L, S) = \max(\|L\|_*, \lambda_{max}\|S\|_1)$  this is straightforward since the set is just the product set of the nuclear norm and  $\ell_1$  norm balls, and efficient projectors onto these are known. In particular, projecting an  $m \times n$  matrix (without loss of generality let  $m \leq n$ ) onto the nuclear norm ball takes  $\mathcal{O}(m^2 n)$  operations, and projecting it onto the  $\ell_1$  ball can be done on  $\mathcal{O}(mn)$  operations using fast median-finding algorithms (Brucker, 1984; Duchi et al., 2008).

For  $\phi_{sum}(L, S) = \|L\|_* + \lambda_{sum}\|S\|_1$ , the projection is no longer straightforward. Nonetheless, the following lemma shows this projection can be efficiently implemented. This lemma appears in van den Berg and Friedlander (2011, Section 9), but supply a proof here since it is not well-known. We begin with a basic proposition:

**Proposition 10** *Projection onto the scaled  $\ell_1$  ball, that is,  $\{x \in \mathbb{R}^d \mid \sum_{i=1}^d \alpha_i |x_i| \leq 1\}$  for some  $\alpha_i > 0$ , can be done in  $\mathcal{O}(d \log(d))$  time.*

We conjecture that fast median-finding ideas could reduce this to  $\mathcal{O}(d)$  in theory, the same as the optimal complexity for the  $\ell_1$  ball. The proof of the proposition follows by noting that the solution can be written in a form depending only on a single scalar parameter, and this scalar can be found by sorting  $(|x_i|/\alpha_i)$  followed by appropriate summations. Armed with the above proposition, we state an important lemma below. For our purposes, we may think of  $S$  as a vector in  $\mathbb{R}^{mn}$  rather than a matrix in  $\mathbb{R}^{m \times n}$ .

**Lemma 11** *Let  $L = U\Sigma V^T$  and  $\Sigma = \text{diag}(\sigma)$ , and let  $(S_i)_{i=1}^{mn}$  be any ordering of the elements of  $S$ . Then the projection of  $(L, S)$  onto the  $\phi_{sum}$  ball is  $(U \text{diag}(\hat{\sigma}) V^T, \hat{S})$ , where  $(\hat{\sigma}, \hat{S})$  is the projection onto the scaled  $\ell_1$  ball  $\{(\sigma, S) \mid \sum_{j=1}^{\min(m,n)} |\sigma_j| + \sum_{i=1}^{mn} \lambda_{sum} |S_i| \leq 1\}$ .*

**Proof** [Sketch of proof] We need to solve

$$\min_{\{(L', S') \mid \phi_{sum}(L', S') \leq 1\}} \frac{1}{2} \|L' - L\|_F^2$$

Alternatively, solve

$$\min_{S'} \left( \min_{\{L' \mid \|L'\|_* \leq 1 - \lambda_{\text{sum}} \|S'\|_1\}} \frac{1}{2} \|L' - L\|_F^2 + \frac{1}{2} \|S' - S\|_F^2 \right).$$

The inner minimization is equivalent to projecting onto the nuclear norm ball, and this is well-known to be soft-thresholding of the singular values. Since it depends only on the singular values, recombining the two minimization terms gives exactly a joint projection onto a scaled  $\ell_1$  ball.  $\blacksquare$

All the references to the  $\ell_1$  ball can be replaced by the intersection of the  $\ell_1$  ball and the non-negative cone, and the projection is still efficient. As noted in Section 3, imposing non-negativity constraints is covered by the gauge results of Theorem 8 and Corollary 9. Therefore, the level set framework can be efficiently applied to this interesting case.

### 3.5 Solving the max ‘flipped’ sub-problem via projected quasi-Newton methods

If we adopt  $\phi_{\max}$  as the regularizer, then the subproblem (**flip-SPCP<sub>max</sub>**) takes the explicit form

$$\begin{aligned} \min_{L,S} \quad & \frac{1}{2} \|L + S - A\|_F^2 \\ \text{s.t.} \quad & \|L\|_* \leq \tau_{\max}, \quad \|S\|_1 \leq \tau_{\max}/\lambda_{\text{sum}}. \end{aligned} \tag{18}$$

The computational bottle-neck is solving this problem quickly, once at each outer iteration. While first-order methods can be used, we can exploit the structure of the objective by using quasi-Newton methods. The main challenge here is that for the  $\|L\|_*$  term, it is tricky to deal with a weighted quadratic term (whereas for  $\|S\|_1$ , we can obtain a low-rank Hessian and solve it efficiently via coordinate descent).

Let  $X = (L, S)$  be the full variable, so we can write the objective function as  $f(X) = \frac{1}{2} \|\mathcal{L}(X) - A\|_F^2$ . To simplify the exposition, we take  $\mathcal{L} = (I, I)$ , but the presented approach applies to general linear operators (including terms like  $\text{Proj}_\Omega$ ). The matrix structure of  $L$  and  $S$  is not yet important here, so we can think of them as reshaped vectors instead of matrices.

The gradient is  $\nabla f(X) = \mathcal{L}^T (\mathcal{L}(X) - A)$ . For convenience, we use  $r(X) = \mathcal{L}(X) - A$  and

$$\nabla f(X) = \begin{pmatrix} \nabla_L f(X) \\ \nabla_S f(X) \end{pmatrix} = \mathcal{L}^T \begin{pmatrix} r(X) \\ r(X) \end{pmatrix}, \quad r_k \equiv r(X_k).$$

The Hessian is  $\mathcal{L}^T \mathcal{L} = \begin{pmatrix} I & I \\ I & I \end{pmatrix}$ . We cannot simultaneously project  $(L, S)$  onto their constraints with this Hessian scaling (doing so would solve the original problem!), since the Hessian removes separability. Instead, we use  $(L_k, S_k)$  to approximate the cross-terms.

The true function is a quadratic, so the following quadratic expansion around  $X_k = (L_k, S_k)$  is exact:

$$\begin{aligned}
 f(L, S) &= f(X_k) + \left\langle \begin{pmatrix} \nabla_L f(X_k) \\ \nabla_S f(X_k) \end{pmatrix}, \begin{pmatrix} L - L_k \\ S - S_k \end{pmatrix} \right\rangle \\
 &\quad + \frac{1}{2} \left\langle \begin{pmatrix} L - L_k \\ S - S_k \end{pmatrix}, \nabla^2 f \begin{pmatrix} L - L_k \\ S - S_k \end{pmatrix} \right\rangle \\
 &= f(X_k) + \left\langle \begin{pmatrix} r_k \\ r_k \end{pmatrix}, \begin{pmatrix} L - L_k \\ S - S_k \end{pmatrix} \right\rangle \\
 &\quad + \frac{1}{2} \left\langle \begin{pmatrix} L - L_k \\ S - S_k \end{pmatrix}, \begin{pmatrix} I & I \\ I & I \end{pmatrix} \begin{pmatrix} L - L_k \\ S - S_k \end{pmatrix} \right\rangle \\
 &= f(X_k) + \left\langle \begin{pmatrix} r_k \\ r_k \end{pmatrix}, \begin{pmatrix} L - L_k \\ S - S_k \end{pmatrix} \right\rangle \\
 &\quad + \frac{1}{2} \left\langle \begin{pmatrix} \mathbf{L} - L_k \\ \mathbf{S} - S_k \end{pmatrix}, \begin{pmatrix} L - L_k + \mathbf{S} - S_k \\ \mathbf{L} - L_k + S - S_k \end{pmatrix} \right\rangle
 \end{aligned}$$

The coupling of the second order terms, shown in bold, prevents direct 1-step minimization of  $f$ , subject to the nuclear and 1-norm constraints. The FISTA method (Beck and Teboulle, 2009a) replaces the Hessian  $\begin{pmatrix} I & I \\ I & I \end{pmatrix}$  with the upper bound  $2 \begin{pmatrix} I & 0 \\ 0 & I \end{pmatrix}$ , which solves the coupling issue, but potentially loses too much second order information. For (**flip-SPCP<sub>sum</sub>**), FISTA is about the best we can do (we actually use SPG (Wright et al., 2009b) which did slightly better in our tests). However, for (**flip-SPCP<sub>max</sub>**)—and for (**lag-SPCP**), which has no constraints but rather non-smooth terms, which can be treated like constraints using proximity operators—the constraints are uncoupled and we can take a “middle road” approach, replacing

$$\left\langle \begin{pmatrix} \mathbf{L} - L_k \\ \mathbf{S} - S_k \end{pmatrix}, \begin{pmatrix} L - L_k + \mathbf{S} - S_k \\ \mathbf{L} - L_k + S - S_k \end{pmatrix} \right\rangle$$

with

$$\left\langle \begin{pmatrix} L - L_k \\ S - S_k \end{pmatrix}, \begin{pmatrix} L - L_k + \mathbf{S}_k - \mathbf{S}_{k-1} \\ \mathbf{L}_{k+1} - \mathbf{L}_k + S - S_k \end{pmatrix} \right\rangle.$$

The first term is decoupled, allowing us to update  $L_k$ , and then this is plugged into the second term in a Gauss-Seidel fashion. In practice, we also scale this second-order term with a number slightly greater than 1 but less than 2 (e.g., 1.25) which leads to more robust behavior. We expect this “quasi-Newton” trick to do well when  $S_{k+1} - S_k$  is similar to  $S_k - S_{k-1}$ .

#### 4. Dual Smoothing and the Proximal Point method

This section describes the approach of the TFOCS algorithm (Becker et al., 2011) and its implementation<sup>2</sup>. The method is based on the proximal point algorithm and handles generic convex minimization problems. The original analysis in Becker et al. (2011) was in terms of convex *cones*, but we re-analyze the method here in terms of extended valued convex *functions*, and find stronger results.

---

2. <http://cvxr.com/tfocs>

Secondly, we compare to alternatives in the literature; the basic ingredients involved in TFOCS are well-known in the optimization community, and there are many variants and applications. We discuss in detail the relationship with the family of preconditioned ADMM methods popularized by [Chambolle and Pock \(2010\)](#). The TFOCS algorithm also motivated the work of [Devolder, Glineur, and Nesterov 2012](#), which promotes an alternative approach that smooths both the primal and the dual. This approach appeared to obtain stronger guarantees, but there is a price to pay, since in the context of sparse optimization, smoothing the primal necessarily yields a less sparse solution. We show that with the improved analysis of TFOCS, TFOCS in fact enjoys the same strong guarantees, while avoiding smoothing the primal.

Finally, we apply this method to RPCA. The TFOCS formulation is flexible and can solve all standard variants of RPCA and SPCP, as well as incorporate non-negativity or other types of additional constraints. We briefly detail how the algorithm can be specialized for the RPCA problem. Even without specializing the algorithm for RPCA, TFOCS has performed well. The results of tests from [Bouwman and Zahzah \(2014\)](#) are that “LSADM ([Goldfarb et al., 2013](#)) and TFOCS ([Becker et al., 2011](#)) solvers seem to be the most adapted ones in the field of video surveillance.”

#### 4.1 General form of our optimization problem

In this section, we provide a general notation that captures all optimization problems of interest. Note that even though we do not explicitly write constraints in this formulation, through the use of extended-value functions we capture constraints, and so in particular can express residual-constrained formulations using this notation.

We consider the following generic problem

$$\min_x \omega(x) + \psi_0(x) + \sum_{i=1}^m \psi_i(\mathcal{L}_i x - b_i) \quad (19)$$

where

- $\omega$  and  $\psi_i$  for  $i = 0, \dots, m$  are proper convex lsc functions on their respective spaces,
- $\omega$  is differentiable everywhere, with Lipschitz continuous gradient; note that we can consider  $\omega(\mathcal{L}x - b)$  trivially, since this is also differentiable,
- $\psi_i$  for  $i = 0, \dots, m$  has an easily computable proximity function,
- $\mathcal{L}_i$  for  $i = 1, \dots, m$  is a linear operator, and  $b_i$  is a constant offset.

We distinguish  $\psi_0$  from  $\psi_i, i \geq 1$ , since  $\psi_0$  is not composed with a linear operator. This is significant since being able to easily compute the proximity operator of  $\psi$  does not imply one can easily compute the proximity operator of  $\psi_i \circ \mathcal{L}_i$  nor of  $\psi_i + \psi_j$ , so we deal with the  $i = 1, \dots, m$  terms specially.

**Remark 12** *Unlike the  $\mathcal{L}_i$  terms, the offsets  $b_i$  can be absorbed into  $\psi_i$ , since if  $\tilde{\psi}(x) = \psi(x - b)$  then  $\text{Prox}_{\tilde{\psi}}(x) = b + \text{Prox}_{\psi}(x - b)$  ([Combettes and Pesquet, 2011](#)). Thus we make these offsets explicit or implicit as convenient.*

RPCA in the general setting (3) can be recovered from the above by setting  $x = (L, S)$ ,  $\psi_0(x) = \phi(L, S)$ ,  $m = 1$  and  $\psi_1 = \rho$  with  $\mathcal{L}_1 x = -L - S$  and  $b_1 = -A$ , and  $\omega = 0$ . In fact,

many convex problems from science and engineering fit into this framework (Combettes and Pesquet, 2011). The strength of this particular model is that it is often easy to decompose a complicated function  $f$  by a finite sum of simple functions  $\psi_i$  composed with linear operators. In this case,  $f$  may not be differentiable, and  $\text{Prox}_f$  need not be easy to compute, so the model allows us to exploit the structure of the smaller building blocks.

## 4.2 Dual smoothing approach

We re-derive the algorithm described in Becker et al. (2011), but from a *conjugate-function* viewpoint, whereas Becker et al. (2011) used a *dual-conic* viewpoint. The later viewpoint is subsumed in the former, and is arguably less elegant.

Consider the problem

$$\min_x f(x) := \psi_0(x) + \sum_{i=1}^m \psi_i(\mathcal{L}_i x - b_i) \quad (20)$$

which is similar to (19) but without the differentiable term  $\omega$ . In addition to our previous assumptions on these functions (convex, lsc, proper), we now assume that at least one minimizer exists (guaranteed if any function is coercive, or any set is bounded).

Our main observation is that instead of solving (20) directly, we can instead use the proximal point method to minimize  $f$ , which exploits the fact that

$$\min_x f(x) = \min_y \left( \min_x f(x) + \frac{\mu}{2} \|x - y\|^2 \right). \quad (21)$$

This fact follows since  $f(x) \leq f(x) + \frac{\mu}{2} \|x - y\|^2$ , and equality is achieved by setting  $y$  to one of the minimizers of  $f$ .

Thus we solve a sequence of problems of the form

$$\min_x f(x) + \frac{\mu}{2} \|x - y\|^2. \quad (22)$$

for a fixed  $y$ . The exact proximal point method is

$$y_{k+1} = \arg \min_x F_k(x) := f(x) + \frac{\mu_k}{2} \|x - y_k\|^2 \quad (23)$$

where  $\mu_k$  is any sequence such that  $\limsup \mu_k < \infty$ , and  $y_0$  is arbitrary. Note that  $F_k$  depends on  $\mu_k$  and  $y_k$ .

The benefit of (22) over (20) is that  $F_k$  is strongly convex, whereas  $f$  need not be, and therefore the dual problem of  $F_k$  is easy to solve, which we will make precise.

Rewriting the objective, and ignoring offset terms  $b_i$  for simplicity (see Remark 12), we have

$$\min_x \underbrace{\psi_0(x) + \frac{\mu}{2} \|x - y\|^2}_{\Phi(x)} + \sum_{i=1}^m \psi_i(\mathcal{L}_i x). \quad (24)$$

For  $i = 1, \dots, m$ , each  $\mathcal{L}_i$  is a linear operator from  $\mathbb{R}^n$  to  $\mathbb{R}^{m_i}$ . We can further simplify notation by defining a linear operator  $\mathbf{L}$  and a vector  $\mathbf{z} \in \mathbb{R}^{\sum_{i=1}^m m_i}$  (e.g.,  $\mathbf{z} = \mathbf{L}(X)$ ) such that

$$\mathbf{L}(x) = \begin{pmatrix} L_1(x) \\ L_2(x) \\ \vdots \\ L_m(x) \end{pmatrix}, \quad \mathbf{z} = \begin{pmatrix} z_1 \\ z_2 \\ \vdots \\ z_m \end{pmatrix}$$

Then define

$$\Psi(\mathbf{z}) = \sum_{i=1}^m \psi_i(z_i), \text{ so } \text{Prox}_{\Psi}(\mathbf{z}) = \begin{pmatrix} \text{Prox}_{\psi_1}(z_1) \\ \text{Prox}_{\psi_2}(z_2) \\ \vdots \\ \text{Prox}_{\psi_m}(z_m) \end{pmatrix} \text{ and } \text{Prox}_{\Psi^*}(\mathbf{z}) = \begin{pmatrix} \text{Prox}_{\psi_1^*}(z_1) \\ \text{Prox}_{\psi_2^*}(z_2) \\ \vdots \\ \text{Prox}_{\psi_m^*}(z_m) \end{pmatrix}. \quad (25)$$

We now rewrite (24) in the following compact representation

$$\min_x \Phi(x) + \Psi(\mathbf{L}x). \quad (26)$$

We are now in position to apply standard Fenchel-Rockafellar duality (Rockafellar, 1970b; Bauschke and Combettes, 2011) to arrive at the dual problem

$$\min_{\mathbf{z}} \underbrace{\Phi^*(\mathbf{L}^*\mathbf{z}) + \Psi^*(-\mathbf{z})}_{q(\mathbf{z})}. \quad (27)$$

Standard constraint qualifications for finite dimensional problems (e.g., Thm. 15.23 and Prop. 6.19x in Bauschke and Combettes (2011)) guarantee a zero duality gap if

$$\text{ri}(\text{dom}\Psi) \cap \mathbf{L}(\text{ri}(\text{dom}\Phi)) \neq \emptyset.$$

The primal problem (26) is not amenable to computation because even though we can calculate the proximity operators of  $\Psi$  and  $\Phi$ , we cannot easily calculate the proximity operator of  $\Psi \circ \mathbf{L}$ . The dual formulation (27) circumvents this because instead of asking for the proximity operator of  $\Phi^* \circ \mathbf{L}^*$ , which is not easy, we will use its gradient, and in this case the linear term causes no issue. We can do this because  $\Phi$  is at least  $\mu$  strongly convex, so we have the following well-known result (see e.g., Prop. 12.60 in Rockafellar and Wets (1998)).

**Lemma 13** *The function  $\Phi^*$  is continuously differentiable and the gradient is Lipschitz continuous with constant  $\mu^{-1}$ , and hence  $\Phi^* \circ \mathbf{L}^*$  is also continuously differentiable with Lipschitz constant  $\|\mathbf{L}\|^2/\mu$ .*

Note we are taking the operator norm of  $\mathbf{L}$ , and  $\|\mathbf{L}\|^2 = \|\mathbf{L}\mathbf{L}^*\| = \sum_{i=1}^n \|\mathcal{L}_i\|^2$ . The actual gradient is can be determined by exploiting the relation

$$\nabla\Phi^*(w) = \partial\Phi^*(w) = \partial\Phi^{-1}(w),$$

which follows from Fenchel's equality (see Rockafellar (1970b, Theorem 23.5)), i.e., if  $x = \nabla\Phi^*(w)$  then  $0 \in \partial\Phi(x) - w$ , so  $x$  minimizes  $\Phi(\cdot) - \langle w, \cdot \rangle$ . Thus

$$\begin{aligned}
 \nabla\Phi^*(w) &= \arg \min_x \Phi(x) - \langle x, w \rangle \\
 &= \arg \min_x \psi_0(x) + \frac{\mu}{2}\|x - y\|^2 - \langle x, w \rangle \\
 &= \arg \min_x \psi_0(x) + \frac{\mu}{2}\|x - (y + w/\mu)\|^2 \\
 &= \text{Prox}_{\psi_0/\mu}(y + w/\mu)
 \end{aligned} \tag{28}$$

so we can calculate the gradient using  $\text{Prox}_{\psi_0}$ . Furthermore, via the chain rule, we have  $\nabla(\Phi^* \circ \mathbf{L}^*)(\mathbf{z}) = \mathbf{L}\nabla\Phi^*(\mathbf{L}^*\mathbf{z})$ .

Thus we have shown that the dual problem (27) is a sum of two functions, one of which has a Lipschitz continuous gradient and the other admits an easily computable proximity operator. Such problems can be readily solved via proximal gradient methods (Combettes and Wajs, 2005) and accelerated proximal gradient methods (Beck and Teboulle, 2009b, 2014).

If strong duality holds, then if  $\mathbf{z}^*$  is a solution of the dual problem,  $x^* = \nabla\Phi^*(\mathbf{L}^*\mathbf{z}^*)$  is the unique solution to the primal problem (cf. Bauschke and Combettes (2011, Prop. 19.3)), and this was used in Becker et al. (2011) to motivate solving the dual. We actually have much stronger results that provide approximate optimality guarantees for approximate dual solutions.

---

**Algorithm 1** TFOCS method (Becker et al., 2011), i.e., FISTA (Beck and Teboulle, 2009b) applied to (27); enforcing  $t_k = 1$  recovers proximal gradient descent

---

**Require:**  $\ell \geq \|\mathbf{L}\|^2/\mu$  bound on Lipschitz constant;  $\mathbf{z}_0$  arbitrary

- 1:  $\mathbf{w}_1 = \mathbf{z}_0, t_1 = 1$ .
  - 2: **for**  $k = 1, 2, \dots$  **do**
  - 3:   Compute  $\tilde{x}_k = \nabla\Phi^*(\mathbf{L}^*\mathbf{w}_k)$  using (28)
  - 4:   Set  $\mathbf{G} = \mathbf{L}\tilde{x}_k = \mathbf{L}\nabla\Phi^*(\mathbf{L}^*\mathbf{w}_k)$
  - 5:    $\mathbf{z}_k = -\text{Prox}_{\ell^{-1}\Psi^*}(-\mathbf{w}_k + \ell^{-1}\mathbf{G})$  using (25) and (7)
  - 6:    $t_{k+1} = \frac{1 + \sqrt{1 + 4t_k^2}}{2} \geq t_k + 1/2$
  - 7:    $\mathbf{w}_{k+1} = \mathbf{z}_k + \frac{t_k - 1}{t_{k+1}}(\mathbf{z}_k - \mathbf{z}_{k-1})$
  - 8: **end for**
- 

We can bound the rate of convergence of the dual objective function  $q$ :

**Theorem 14 (Thm. 4.4 in Beck and Teboulle (2009b))** *The sequence  $(\mathbf{z}_k)$  generated by Algorithm 1 satisfies*

$$q(\mathbf{z}_k) - \min_{\mathbf{z}} q(\mathbf{z}) \leq \frac{2\ell d_0^2}{k^2}$$

where  $d_0$  is the distance from  $\mathbf{z}_0$  to the optimal set.

From this, we can recover a remarkable bound on the primal sequence.

**Theorem 15 (Thm. 4.1 in Beck and Teboulle (2014))** *Let  $(x_k)$  be the sequence generated by*

$$x_k = \nabla\Phi^*(\mathbf{L}^*\mathbf{z}_k)$$

(similar to  $\tilde{x}_k$  but evaluated at  $\mathbf{z}_k$  not  $\mathbf{w}_k$ ). Let  $x^*$  be the (unique) optimal point to (26). Then

$$\frac{\mu}{2} \|x_k - x^*\|^2 \leq q(\mathbf{z}_k) - \min_{\mathbf{z}} q(\mathbf{z})$$

for any point  $\mathbf{z}_k$ , and hence for  $(\mathbf{z}_k)$  from Algorithm 1,

$$\|x_k - x^*\| \leq \frac{2\sqrt{\ell}d_0}{\sqrt{\mu k}}. \quad (29)$$

Note that in practice, one typically uses  $\tilde{x}_k$  for any convergence tests, since it is a by-product of computation, whereas  $x_k$  is expensive to compute. Since  $0 \leq (t_k - 1)/t_{k+1} < 1$  for  $t_k \in [1, \infty)$ , then if  $\mathbf{z}_k$  converges, it follows that  $\mathbf{w}_k$  converges to the same limit, so asymptotically  $x_k \simeq \tilde{x}_k$ .

The result of the above theorem holds regardless of how the sequence  $(\mathbf{z}_k)$  is generated, so if the dual method has better than worst-case convergence (or if an acceleration such as a line search is used), then the primal sequence enjoys the same improvements.

Since  $\sqrt{\ell} = \|\mathbf{L}\|/\sqrt{\mu}$ , combining with the other factor of  $1/\sqrt{\mu}$  shows that  $\|x_k - x^*\| \propto 1/(\mu k)$ , so choosing  $\mu$  large leads to fast convergence (since the dual problem is very smooth). The trade-off is that the outer loop (the proximal point method) will converge more slowly with  $\mu$  large.

### 4.3 Comparison with literature

**Dual methods** The proposed method has been formulated in several contexts; part of the novelty of Becker et al. (2011) is the generality of the method and pre-built function routines from which a wide variety of functions could be constructed. The basic concepts of duality and smoothing are widely used, and using duality to avoid difficult affine terms goes back to Uzawa’s method (see (Ciarlet, 1989)) and the general concept of *domain decomposition*.

More recent and specific approaches include those of (Combettes et al., 2010; Liu et al., 2011; Malgouyres and Zeng, 2009; Necoara and Suykens, 2008) which particularly deal with signal processing problems. The work Combettes et al. (2010) considers a single smoothed problem, not the full proximal point sequence, and uses proximal gradient descent to solve the dual. They establish convergence of the primal variable but without a bound on the convergence rate. Explicit use of the proximal point algorithm is mentioned in Liu et al. (2011), which focuses on the nuclear norm minimization problem, but uses Newton-CG methods, which requires a third level of algorithm hierarchy and good heuristic values for stopping criteria of the conjugate-gradient method. The algorithm SDPNAL (Zhao et al., 2010) is similar to Liu et al. (2011) and uses a Newton-CG augmented Lagrangian framework to solve general semi-definite programs (SDP). The work of Malgouyres and Zeng (2009) focuses on a more specific version of the problem but contains the same general ideas, and has inner and outer iterations. The algorithm in Necoara and Suykens (2008) focuses on standard ADMM settings that have non-trivial linear terms, and smooths the dual problem; they follow Nesterov (2005) and have specific complexity bounds when the appropriate constraint set is compact.

**Primal-dual methods** Another method to remove effects of the linear terms  $\mathcal{L}_i$  is to solve a primal-dual formulation. Many of these are based on duplicating variables into a product space and then enforcing *consensus* of the duplicated variables. This can replace many terms, such as  $\sum_{i=1}^m \psi_i(\mathcal{L}_i x)$ , with two generalized functions, which is inherently easier, since it is often amenable to the Douglas-Rachford algorithm (Combettes and Pesquet, 2007). Specific examples of this

approach are (Combettes and Pesquet, 2012; Combettes, 2013; Becker and Combettes, 2014; Boj et al., 2013b,a, 2015; Boj and Csetnek, 2014). The paper by Briceo-Arias and Combettes (2011) is slightly unique in that it reformulates the primal-dual problem into one that can be solved by the obscure forward-backward-forward algorithm of Tseng (the forward-backward algorithm does not apply since in the primal-dual setting, Lipschitz continuity does not imply co-coercivity).

Another main line of primal-dual methods was motivated in Esser et al. (2009) as a preconditioned variant of ADMM and then analyzed in Chambolle and Pock (2010), and an improved analysis by He and Yuan (2012a) allowed a generic formulation to be proposed independently by Vũ (2013); Condat (2013). In more particular settings, it is known as *linearized* ADMM or primal-dual hybrid gradient (PDHG), and has seen a recent surge of interest and analysis (Tran-Dinh and Cevher, 2014; He and Yuan, 2012b; Li et al., 2014; Ren and Lin, 2013; Wang and Yuan, 2012; Yang and Yuan, 2013; Zhang et al., 2010; Yang and Zhang, 2011; Goldstein et al., 2013). Several recent survey papers (Cevher et al., 2014; Komodakis and Pesquet, 2015) review these algorithms in more detail.

The PDHG has not been applied specifically to the RPCA problem to our knowledge. The next section describes this method in more detail.

**Detailed comparison with PDHG** On certain classes of problems, our approach is quite similar to the PDHG approach. Consider the following simplified version of (20):

$$\min_x \psi_0(x) + \psi_1(\mathcal{L}x - b)$$

At each step of the proximal point algorithm, we minimize the above objective perturbed by  $\mu/2\|x - y\|^2$ , where  $\mu > 0$  is arbitrary. Applying FISTA to the dual problem leads to steps of the following form:

$$\begin{aligned} x_{k+1} &= \arg \min_x \psi_0(x) - \langle \bar{z}, \mathcal{L}x - b \rangle + \frac{\mu}{2} \|x - y\|^2 \\ z_{k+1} &= \arg \min_z \psi_1^*(z) - \langle z, \mathcal{L}x_{k+1} \rangle + \frac{1}{2t} \|z - z_k\|^2 \\ \bar{z} &= z_{k+1} + \theta_k (z_{k+1} - z_k) \end{aligned}$$

where  $\theta_k = (t_k - 1)/t_{k-1}$  as in Algorithm 1 (and  $\lim_{k \rightarrow \infty} \theta_k = 1$ ). We require the stepsize  $t$  to satisfy  $t \leq \mu/\ell^2$ .

For the PDHG method, pick stepsizes  $\tau\sigma < 1/\ell^2$ . There is no outer loop over  $y$ , and the full algorithm is:

$$\begin{aligned} z_{k+1} &= \arg \min_z \psi_1^*(z) - \langle z, \mathcal{L}\bar{x} \rangle + \frac{1}{2\sigma} \|z - z_k\|^2 \\ x_{k+1} &= \arg \min_x \psi_0(x) - \langle \bar{z}, \mathcal{L}x - b \rangle + \frac{1}{2\tau} \|x - x_k\|^2 \\ \bar{x} &= x_{k+1} + \theta (x_{k+1} - x_k) \end{aligned}$$

with  $\theta = 1$  (see Algorithm 1 in Chambolle and Pock (2010)).

The two algorithms are extremely similar, the main differences being that the TFOCS approach updates  $y$  occasionally, while PDHG updates  $y = x_k$  every iteration of the inner algorithm and thus avoids the outer iteration completely. The lack of the outer iteration is an advantage, mainly since it avoids the issue of a stopping criteria. However, the advantage of an inner iteration is that we

can apply an accelerated Nesterov method, which can only be done in the PDHG if one has further assumptions on the objective function.

We present a numerical comparison of the two algorithms applied to RPCA in Figures 2 and 3.

**Detailed comparison with double-smoothing approach** For minimizing smooth but not strongly convex functions  $f$ , classical gradient descent generates a sequence of iterates  $(x_k)$  such that the objective converges at rate  $f(x_k) - \min_x f(x) \leq \mathcal{O}(1/k)$ , and  $(x_k)$  itself converges, with  $\|\nabla f(x_k)\| \leq \mathcal{O}(1/\sqrt{k})$ . The landmark work of Nesterov (1983) showed that a simple acceleration technique similar to the heavy-ball method generates a sequence  $(x_k)$  such that  $f(x_k) - \min_x f(x) \leq \mathcal{O}(1/k^2)$ , although there are no guarantees about convergence of the sequence<sup>3</sup>  $(x_k)$  nor strong bounds on  $\|\nabla f(x_k)\|$ . Note that our dual scheme uses FISTA (Beck and Teboulle, 2009a) which is a generalization of Nesterov’s scheme; we refer to any such scheme with  $\mathcal{O}(1/k^2)$  as “accelerated”.

Defining an  $\epsilon$ -solution to be a point  $x$  such that  $f(x) - \min_x f(x) \leq \epsilon$ , we see that it takes  $\mathcal{O}(1/\epsilon)$  and  $\mathcal{O}(1/\sqrt{\epsilon})$  iterations to reach such a point using the classical and accelerated gradient descent schemes, respectively.

In 2005 Nesterov introduced a smoothing technique (Nesterov, 2005) which applies to minimizing non-smooth functions over compact sets. A naive approach would use sub-gradient descent, in which the worst-case convergence of the objective is  $\mathcal{O}(1/\sqrt{k})$ . By smoothing the primal function by a sufficiently small fixed amount, then using the compact constraints, the smooth function differs from the original function by less than  $\epsilon/2$ . One can then apply Nesterov’s accelerated method which generates an  $\epsilon/2$ -optimal point (to the smoothed problem, and hence  $\epsilon$  optimal to the original problem) in  $\mathcal{O}(\ell/\sqrt{\epsilon})$  iterations. The catch is that  $\ell$  is the Lipschitz constant of the smoothed objective, which is proportional to  $\epsilon^{1/2}$ , so the overall convergence rate is  $\mathcal{O}(1/\epsilon)$ , which is still better than the subgradient schemes that would take  $\mathcal{O}(1/\epsilon^2)$ .

The aforementioned smoothing technique is an alternative to our approach, but the two are not directly comparable, since we do not assume the objective has the same form, nor is our domain necessarily bounded. Furthermore, smoothing the primal objective can have negative consequences. For example, it is common to solve  $\ell_1$  regularized problems in order to generate sparse solutions. Our dual-smoothing technique keeps the primal non-smooth and therefore still promotes sparsity, whereas a primal-smoothing technique would replace  $\ell_1$  with the Huber function, and this does not promote sparsity; see Fig. 1 in Becker et al. (2011).

Another option is the *double-smoothing* technique proposed by Devolder et al. (2012). This is the approach most similar with our own. Like our approach, a strongly convex term is added to the primal problem in order to make the dual problem smooth, and then the dual problem is solved with an accelerated method. Departing from our approach, they additionally smooth the primal as well (as in Nesterov (2005)), which makes the dual problem strongly convex. The reason for this is subtle. Without the strong convexity in the dual (i.e., our approach), we only have a bound on the dual objective function. To translate this into a bound on the primal variable, measured in terms of objective function or distance to the feasible set, requires using the gradient of the dual variable. As mentioned above, accelerated methods have faster rates of convergence in the objective but not of the gradients. For this reason, one must resort to a classical gradient descent method which has slower rates of convergence.

---

3. There is no experimental evidence that the sequence does not converge, and indeed a recent preprint shows that a slight modification of the algorithm can guarantee convergence(Chambolle and Dossal, 2014)

Making the dual problem strongly convex allows the use of special variants of Nesterov’s accelerated method (see [Nesterov \(2004\)](#)) which converge at a linear rate, and, importantly, so do the iterates and their gradients. The convergence is in terms of the smooth and perturbed problem, so the size of these perturbations is controlled in such a manner (again, the domains are assumed to be bounded) such that one recovers a  $\mathcal{O}(1/\epsilon \log(1/\epsilon))$  convergence rate.

The analysis of [Devolder et al. \(2012\)](#) suggests that our method of single smoothing is flawed, but this seems to be an artifact of previous analysis. Using [Theorem 15](#), which is a recent result, we have a rate on the convergence of the primal sequence, rather than on its objective value or distance to optimality. In many situations this is a stronger measure of convergence, depending on the purpose of solving the optimization problem. For robust PCA, the distance to the true solution is indeed a natural metric, whereas sub-optimality of the objective function is rather artificial, and distance to the feasible set depends on the choice of model parameters which maybe somewhat arbitrary.

Furthermore, the lack of bounds on the iterate *sequence* generated by an accelerated method, which was the issue in the analysis of [Devolder et al. \(2012\)](#), is mainly a theoretical one, since in most practical situations, the variables and their gradients do appear to converge at a fast rate. Our situation is also different since the constraints need not be compact, and we use the proximal point method to reduce the effect of the smoothing.

#### 4.4 Effect of the smoothing term

The next section discusses convergence of the proximal point method, but we first discuss the phenomenon that sometimes, the proximal point method converges to the exact solution in a finite number of iterations. This case is not covered by classical exact penalty results ([Bertsekas et al., 2003](#)), which only apply when the perturbation is non-smooth (e.g.,  $\|x - y\|$ ), whereas we use a smooth perturbation  $\|x - y\|^2$ .

Whenever the functions and constraints are polyhedral, such as for linear programs, finite convergence (or the “exact penalty” property) will occur. This was known since the 1970s; see Prop. 8 in [Rockafellar \(1976\)](#) and ([Mangasarian and Meyer, 1979](#); [Poljak and Tretjakov, 1974](#); [Bertsekas, 1975](#)). The special case of noiseless basis pursuit was recently analyzed in [Yin \(2010\)](#) using different techniques. More general results, allowing a range of penalty functions, were proved in [Friedlander and Tseng \(2007\)](#).

For non-polyhedral problems, exact penalty does not occur in general. For example, one can construct an example of nuclear norm minimization which does not have the exact penalty property. However, under additional assumptions that are typical to guarantee exact recovery in the sense of [Candés and Plan \(2010\)](#), it is possible to obtain exact penalty results. Research in this is motivated by the popularity of the ([Cai et al., 2010](#)) algorithm, which is a special case of the TFOCS framework applied to matrix completion. Results are in [Lai and Yin \(2013\)](#), as well as [Zhang et al. \(2012\)](#) (and the correction [You et al. \(2013\)](#)) which also provides results for the RPCA problem in particular. Some results on generalizations to tensors are also available [Shi et al. \(2013\)](#).

#### 4.5 Convergence

**Certificates of accuracy of the sub-problem** For solving the smoothed sub-problem  $\min_x F_k(x)$ , we assume the proximity operator of each  $\psi_i$  is easy to compute, and given this, it is reasonable to expect that it is easy to compute a point in  $\partial\psi_i$  as well. Furthermore, since the algorithm computes the effect of the linear operators on the current iterate, it may be possible to reuse previously computed

values. Thus, computing a point in  $\partial F_k$  may be relatively cheap since it is just the sum of the  $\partial\psi_i$  composed with the appropriate linear operators. We can now obtain accuracy guarantees via the following proposition.

**Proposition 16** (*Rockafellar, 1976, Prop. 3*) *Let  $y = \arg \min_x F_k(x)$ , then for all points  $x$  and all  $d \in \partial F_k(x)$ ,*

$$\|x - y\| \leq \mu_k^{-1} \|d\|. \quad (30)$$

**Convergence of the proximal point method** The convergence of the proximal point method is well-understood, but we are particularly interested in the case when the update step is computed inaccurately. There has been recent work on this (see e.g. (M. Schmidt, 2011; Villa et al., 2013; Devolder et al., 2011)) but often under the assumption that the computed point is feasible, i.e., it is inside  $\text{dom} f$ . Using the dual method, this cannot be guaranteed in general (though it certainly applies to many special cases). One can apply the analysis of gradient descent from (Devolder et al., 2011) to the proximal point algorithm (viewed as gradient descent on the Moreau-Yosida envelope), and compute an inexact gradient in the sense that the primal point is the exact gradient of a perturbed point. This perturbed point is based on the sub-optimality of the dual variable (see (28)), which, per the discussion of Devolder et al. (2012) above, does not have a bounded converge rate when using an accelerated algorithm, and hence we do not pursue this line of analysis.

We start with an extremely broad theorem that guarantees convergence under minimal assumptions, albeit without an explicit convergence rate:

**Theorem 17** (*Rockafellar, 1976, Thm. 1*) *The approximate proximal point method defined by*

$$\begin{aligned} \tilde{y}_{k+1} &= \arg \min F_k(x) \\ y_{k+1} &\text{ any point satisfying } \|y_{k+1} - \tilde{y}_{k+1}\| \leq \epsilon_k \end{aligned}$$

*with  $\sum_{k=1}^{\infty} \epsilon_k < \infty$ ,  $y_0$  arbitrary,  $F_k$  as defined in (23), and  $\limsup_{k \rightarrow \infty} \mu_k < \infty$ , will generate a sequence  $\{y_k\}$  that converges to a minimizer of  $f$ .*

We note that the boundedness of iterates follows by our assumption that a minimizer exists; in infinite dimensions, convergence is in the weak topology. To guarantee  $\|y_{k+1} - \tilde{y}_{k+1}\| \leq \epsilon_k$ , we can either bound this *a priori* using Thm. 15, or we can bound it *a posteriori* by explicitly checking using Prop. 16.

We state a second theorem that guarantees local linear convergence under standard assumptions. This assumption is that there is a unique solution to  $\min f(x)$  and that  $f$  has sufficient curvature nearby; it is related to the standard second-order sufficiency condition, but slightly weaker. See Rockafellar (1976) for an early use, and Burke and Qian (1997) for a more recent discussion.

**Assumption 1** *There is a unique solution  $x^*$  to  $\min f(x)$ , i.e.,  $\partial f^{-1}(0) = x^*$ ; and  $\partial f^{-1}$  is locally Lipschitz continuous at 0 with constant  $a$ , i.e., there is some  $r$  such that  $\|w\| \leq r$  implies  $\|x - x^*\| \leq a\|w\|$  whenever  $x \in \partial f^{-1}(w)$ .*

Recall that via basic convex analysis,  $0 \in \partial f(x^*)$ . Finding  $\arg \min F_k(x)$  is the same as computing the proximity operator  $P_k \stackrel{\text{def}}{=} (I + \mu_k^{-1} \partial f)^{-1}$ . Define  $Q_k = I - P_k$ , then we have that  $P_k$  (and  $Q_k$ ) are firmly non-expansive (Moreau, 1965; Bauschke and Combettes, 2011), meaning

$$\forall x, x', \|P_k(x) - P_k(x')\|^2 + \|Q_k(x) - Q_k(x')\|^2 \leq \|x - x'\|^2.$$

Furthermore,  $x^* = P_k(x^*)$  (this is independent of  $\mu_k$ ), and  $Q_k(x^*) = 0$ . Now, we state a novel theorem, where for simplicity we have assumed  $\mu_k \equiv \mu \neq 0$ :

**Theorem 18** *Under Assumption 1, the approximate proximal point method defined by*

$$\begin{aligned} \tilde{y}_{k+1} &= \arg \min F_k(x) \\ y_{k+1} &\text{ any point satisfying } \|y_{k+1} - \tilde{y}_{k+1}\| \leq (\gamma/2)^k \end{aligned}$$

with

$$\gamma = \frac{a}{\sqrt{a^2 + \mu^{-2}}} < 1$$

generates a sequence  $(y_k)$  that converges linearly to  $x^*$  for all  $k$  sufficiently large, and with rate  $\gamma$ .

**Proof** Note that we have defined  $\tilde{y}_{k+1} = P_k(y_k)$ . Observe that the assumption of Theorem 17 holds since the errors are clearly summable, hence  $(y_k)$  converges, and  $\|y_{k+1} - y_k\| \rightarrow 0$ , so this is arbitrarily small for  $k$  sufficiently large. We also have

$$\|Q_k(y_k)\| = \|y_k - P_k(y_k)\| \leq \|y_k - y_{k+1}\| + \|y_{k+1} - P_k(y_k)\|$$

and both the terms on the right side go to zero. By basic convex analysis (e.g., Prop. 1a in Rockafellar (1976)),

$$P_k(y_k) \in \partial f^{-1}(\mu Q_k(y_k))$$

and so for  $k$  large enough (say,  $k \geq k_0$ ), we are in the Lipschitz region of the assumption, so

$$\|P_k(y_k) - x^*\| \leq a\|Q_k(y_k)\|. \quad (31)$$

Now using the firmly non-expansiveness and properties of  $x^*$  mentioned above,

$$\|x^* - P_k(y_k)\|^2 + \|Q_k(y_k)\|^2 \leq \|x^* - y_k\|^2 \quad (32)$$

so combining (31) with (32) gives

$$\|x^* - P_k(y_k)\| \leq \gamma\|x^* - y_k\|$$

which in effect proves the eventual linear convergence in the exact case where  $y_{k+1} = P_k(y_k)$  (up to this point, the proof follows Thm. 2 from Rockafellar (1976)).

Now bound

$$\begin{aligned} \|y_{k+1} - x^*\| &\leq \|y_{k+1} - P_k(y_k)\| + \|P_k(y_k) - x^*\| \\ &\leq (\gamma/2)^k + \gamma\|y_k - x^*\| \\ &\leq (\gamma/2)^k + \gamma \left( (\gamma/2)^{k-1} + \gamma\|y_{k-1} - x^*\| \right) \\ &\vdots \\ &\leq \gamma^k \sum_{i=k_0}^k 2^{-i} + \gamma^{k+1-k_0}\|y_{k_0} - x^*\| \\ &\leq \gamma^k \left( 1 + \gamma^{1-k_0}\|y_{k_0} - x^*\| \right) \end{aligned}$$

which proves our result. ■

Again, we can certify that  $y_{k+1} \simeq P_k(y_k)$  either use Thm. 15, or we can bound it *a posteriori* by explicitly checking using Prop. 16. Since the linear convergence only occurs locally, it is not possible to provide an overall iteration-complexity of the inner and outer iterations (it is possible with further assumptions on  $f$ , such as  $f$  having full domain; see Becker (2011)). Without some form of strong convexity near the solution, it is generally not possible to bound the rate on the iterates, but rather only bound the rate of the objective function, and this is not possible with the dual approach since the point may not be feasible.

If we assume that the linear convergence occurs globally, then we can combine this with our complexity bound on the sub-problem from (29). Converting that rate to our new notation, and using  $j$  to index the inner loop, and setting the initial dual variable  $\mathbf{z}_0$  to the one corresponding to  $y_k$ , we have

$$\|x_j - P_k(y_k)\| \leq 2 \frac{\|\mathbf{L}\| d_k}{\mu \cdot j}$$

where  $d_k$  is the distance from  $\mathbf{z}_0$  (corresponding to  $y_k = \nabla\Phi^*(\mathbf{L}^*\mathbf{z}_0)$ ) to the optimal set of dual solutions. Bounding this explicitly can be done in some cases (see Bruer et al. (2014)), but for the sake of analysis we will simply assume  $d_k$  is upper-bounded by some  $d$ .

#### 4.6 Solving the dual problem efficiently in the case of RPCA

For solving (2), we set  $\psi_0(L, S) = \|L\|_* + \lambda\|S\|_1$  and  $\psi_1(\mathcal{L}(L, S) - A) = \chi_{\{0\}}(L + S - A)$  to enforce the constraint exactly. In this case,  $\psi_1^*$  is the constant function, and so  $\text{Prox}_{\psi_1^*}$  is the identity — that is to say, the dual problem is unconstrained.

In that case, instead of using FISTA to solve the dual, one may use techniques from *unconstrained* optimization, such as non-linear conjugate gradient and L-BFGS (Nocedal and Wright, 2006). These algorithms work extremely well in practice. We do not go into further detail since we find the exact constraint formulation of RPCA to be artificial. With inequality constraints, the dual problem becomes non-smooth so it is necessary to use a proximal gradient method. Due to the cost of the objective function, it may be worthwhile to use quasi-Newton projected gradient methods such as that of Schmidt et al. (2009).

## 5. Numerical Experiments

### 5.1 Numerical results for TFOCS

To highlight the flexibility of TFOCS, we consider a background subtraction problem of a surveillance video in which we do not wish to enforce  $A = L + S$  but instead we wish to separate  $A$  into components up to the quantization level. The video  $A$  is quantized to integer values between 0 and 255, so we can think of this as being the quantized version of some real-valued video  $\hat{A}$ , and thus  $\|\hat{A} - A\|_\infty \leq 0.5$  since the quantized version is rounded to the nearest integer. Hence we solve the following:

$$\min_{L, S} \phi_0(L, S) = \|L\|_* + \lambda\|S\|_1 \quad \text{s.t.} \quad \|A - L - S\|_\infty \leq 0.5. \quad (33)$$

In the TFOCS software (written in MATLAB), we work with the primal variable  $\mathbf{x} = \{L, S\}$ , and one specifies the function  $\psi_0$  in the term `obj` like

```
obj = { prox_nuclear(1), prox_l1(lambda) };
```

Next we encode  $\psi_1$  and  $\mathcal{L}_1$  and  $b_1$ . The linear term, applied to  $X=\{L, S\}$ , is  $\mathcal{L}_1 = [I, I]$ , and the offset is  $b_1 = -A$ . This is encoded as

```
affine = { 1, 1, -A };
```

and  $\psi_1$  is represented implicitly by giving its conjugate. For standard equality constrained RPCA, the constraint is  $A - L - S = 0$ , so  $\psi_1$  is the indicator function of the set  $\{0\}$ , and the conjugate of this is the function that is constant everywhere, so its proximity operator is the identity (i.e., projection on  $\mathbb{R}^n$ ). This is written

```
dualProx = proj_Rn
```

If instead we wish to solve (33), then  $\psi_1$  is the indicator function of the  $\ell_\infty$  ball of radius  $1/2$ , and so its conjugate is  $1/2 \|\cdot\|_1$ , which is written

```
dualProx = prox_l1(0.5);
```

The code can then be called as follows:

```
X = tfocs_SCD( obj, affine, dualProx, mu, X0 );
```

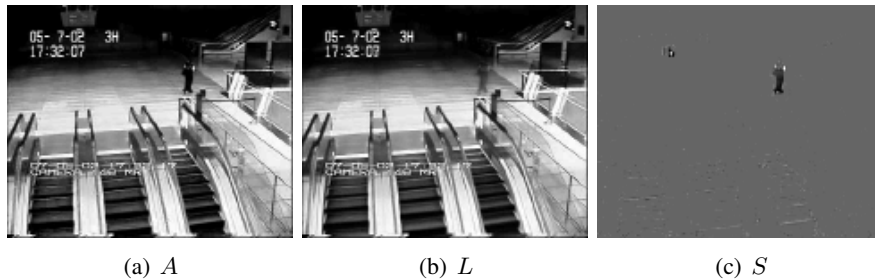


Figure 1: Frame 110 from the movie, showing original  $A$ , low-rank  $L$  and sparse  $S$  components

More detailed code is available as a demo at <sup>4</sup>; the video data is from <sup>5</sup>. Results are shown in Fig. 1. Although the walking person is correctly identified in the  $S$  component, a small amount of the person appears in  $L$ . However, it is remarkable that the low-rank component mostly captures the moving escalator, which is a feat that most background subtraction cannot do without a specially targeted algorithm.

**Comparison with PDHG** As discussed in §4.3, the primal-dual hybrid gradient (PDHG) method is similar to the TFOCS algorithm. In TFOCS, one controls the value of  $\mu$  and then runs the proximal point algorithm, and the sub-problem is solved by FISTA (or variants) that use linesearch techniques and therefore do not need a stepsize. In PDHG, there is no line search, but there are two stepsizes  $\tau$  and  $\sigma$  which are linked in the fashion  $\tau\sigma < 1/\ell^2$ . Larger stepsizes generally lead to better performance, so by insisting  $\tau\sigma = 0.99/\ell^2$ , there is only one effective parameter choice.

Using a version of the same escalator film discussed in the previous section, we compare PDHG and TFOCS on (SPCP<sub>sum</sub>). In TFOCS, we encode this with

4. <http://cvxr.com/tfocs/demos/rpca/>

5. [http://perception.i2r.a-star.edu.sg/bk\\_model/bk\\_index.html](http://perception.i2r.a-star.edu.sg/bk_model/bk_index.html)

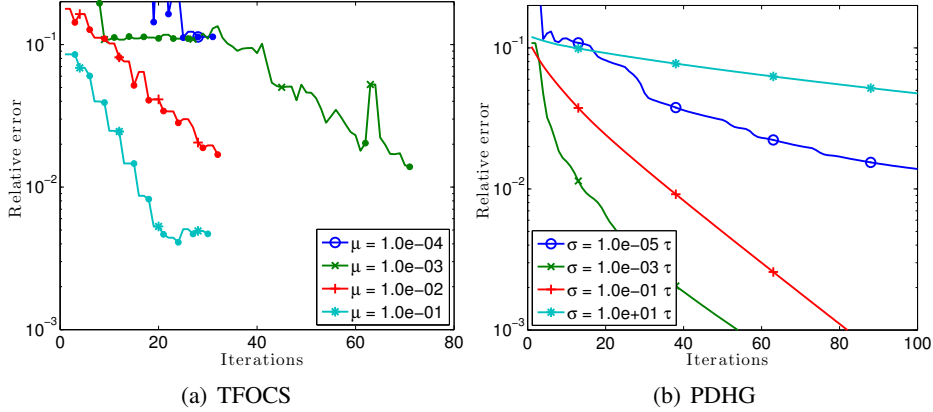


Figure 2: Convergence plots on the elevator data, for various parameter values. The small dots in the TFOCS plot show where the proximal point algorithm took another outer step.

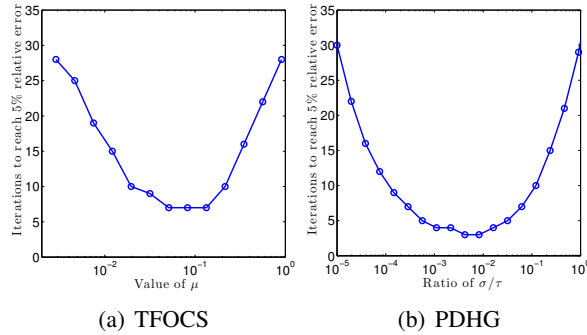


Figure 3: Number of iterations to reach a fixed tolerance, as function of parameter value

```
dualProx = prox_l2(epsilon);
```

The parameters  $\epsilon$  and  $\lambda$  were chosen by running the quasi-Newton solver on **(lag-SPCP)** and tuning by hand until results looked acceptable. Running the special purpose solver gives a very accurate reference answer. From the solution to **(lag-SPCP)**, one can infer  $\epsilon$  and  $\lambda_{\text{sum}}$ .

Neither method is specific for RPCA problems, so we do not expect cutting-edge performance, but we do see reliable performance, and the ability to adapt to variations in the model. We focus on parameter selection. Both methods perform roughly equally, and both are strongly dependent on the parameter choice. A major weakness of all current methods is lack of guidance for choosing parameters in practice; the effort of [Pock and Chambolle \(2011\)](#) to find good values resulted in mixed success. The software TFOCS automatically rescales variables in order to make all  $\mathcal{L}_i$  terms have the same spectral norm, which has a small beneficial effect.

Fig. 2 shows the decay of the relative error  $\sqrt{\|L - L_0\|_F^2 + \|S - S_0\|_F^2} / \sqrt{\|L_0\|_F^2 + \|S_0\|_F^2}$  where  $(L_0, S_0)$  is the accurate reference solution computed via the quasi-Newton algorithm. TFOCS has the advantage that the sub-problems can use a fast solver with a good linesearch, but the disadvantage that with the two levels of iterations, the inner iteration must be terminated at the right

time. If it is stopped too early, the solution is not accurate enough, while if it is stopped too late, the algorithm wastes time on finding a very precise answer to a useless intermediate problem.

Fig. 3 shows the number of iterations required to reach a fixed tolerance. Confirming the behavior in the previous figure, it is clear that convergence can be rapid for good parameter choices, and slow for poor parameter choices.

## 5.2 Numerical results for quasi-Newton algorithm

We compare new algorithms and formulations to PSPG (Aybat et al., 2013), NSA (Aybat and Iyengar, 2013), and ASALM (Tao and Yuan, 2011)<sup>6</sup>. We modified the other software as needed for testing purposes. PSPG, NSA and ASALM all solve (SPCP<sub>sum</sub>), but ASALM has another variant which solves (lag-SPCP) so we test this as well. All three programs also use versions of PROPACK from Becker and Candès (2008) to compute partial SVDs. We measure error as a function of time, since cost of a single iteration can vary among the solvers. To fairly compare all the algorithms in the simulated experiments, we measure the (relative) error of a trial solution  $(L, S)$  to a reference solution  $(L^*, S^*)$  as  $\|L - L^*\|_F / \|L^*\|_F + \|S - S^*\|_F / \|S^*\|_F$ . Time to compute this error is accounted for (so does not factor into the comparisons). Finally, since stopping conditions are solver dependent, we show plots of error vs time. All tests are done in Matlab and the dominant computational time was due to matrix multiplications for all algorithms; all code was run in the same quad-core 1.6 GHz i7 computer.

For our implementations of the (flip-SPCP<sub>max</sub>), (flip-SPCP<sub>sum</sub>) and (lag-SPCP), we use a randomized SVD (Halko et al., 2011). Since the number of singular values needed is not known in advance, the partial SVD may be called several times (the same is true for PSPG, NSA and ASALM). Our code limits the number of singular values on the first two iterations in order to speed up calculation without affecting convergence. Since the projection required by (flip-SPCP<sub>sum</sub>) makes a partial SVD difficult, so we use Matlab’s dense SVD routine.

### 5.2.1 SYNTHETIC TEST WITH EXPONENTIAL NOISE

We first provide a test with generated data. The observations  $A \in \mathbb{R}^{m \times n}$  with  $m = 400$  and  $n = 500$  were created by first sampling a rank 20 matrix  $A_0$  with random singular vectors (i.e., from the Haar measure) and singular values drawn from a uniform distribution with mean 0.1, and then adding exponential random noise to the entire matrix (with mean equal to one tenth the median absolute value of the entries of  $A_0$ ). This exponential noise, which has a longer tail than Gaussian noise, is expected to be captured partly by the  $S$  term and partly by the error term  $\|L + S - A\|_F$ .

Given  $A$ , the reference solution  $(L^*, S^*)$  was generated by solving (lag-SPCP) to very high accuracy; the values  $\lambda_L = 0.25$  and  $\lambda_S = 10^{-2}$  were picked by hand tuning  $(\lambda_L, \lambda_S)$  to find a value such that both  $L^*$  and  $S^*$  are non-zero. The advantage to solving (lag-SPCP) is that knowledge of  $(L^*, S^*, \lambda_L, \lambda_S)$  allows us to generate the parameters for all the other variants, and hence we can test different problem formulations.

With these parameters,  $L^*$  was rank 17 with nuclear norm 6.754,  $S^*$  had 54 non-zero entries (most of them positive) with  $\ell_1$  norm 0.045, the normalized residual was  $\|L^* + S^* - A\|_F / \|A\|_F = 0.385$ , and  $\varepsilon = 1.1086$ ,  $\lambda_{\text{sum}} = 0.04$ ,  $\lambda_{\text{max}} = 150.0593$ ,  $\tau_{\text{sum}} = 6.7558$  and  $\tau_{\text{max}} = 6.7540$ .

6. PSPG, NSA and ASALM available from the experiment package at <http://www2.ie.psu.edu/aybat/codes.html>

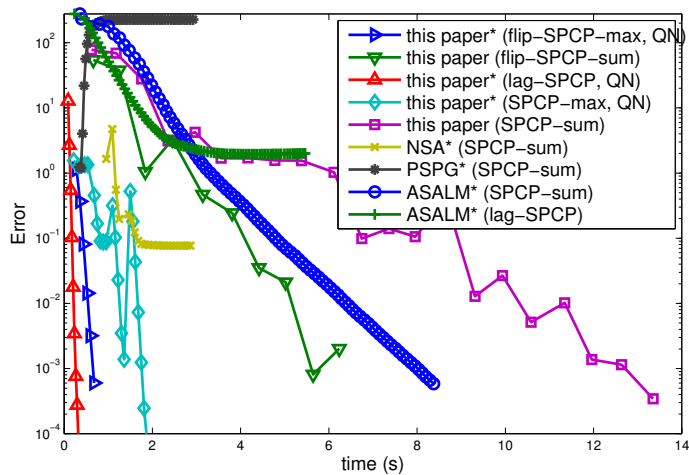


Figure 4: The exponential noise test. The asterisk in the legend means the method uses a fast SVD (i.e., randomized SVD).

Results are shown in Fig. 4. Our methods for (**flip-SPCP<sub>max</sub>**) and (**lag-SPCP**) are extremely fast, because the simple nature of these formulations allows the quasi-Newton acceleration scheme of Section 3.5. In turn, since our method for solving (**SPCP<sub>max</sub>**) uses the variational framework of Section 3 to solve a sequence of (**flip-SPCP<sub>max</sub>**) problems, it is also competitive (shown in cyan in Figure 4). The jumps are due to re-starting the sub-problem solver with a new value of  $\tau$ , generated according to (14).

Our proximal gradient method for (**flip-SPCP<sub>sum</sub>**), which makes use of the projection in Lemma 11, converges more slowly, since it is not easy to accelerate with the quasi-Newton scheme due to variable coupling, and it does not make use of fast SVDs. Our solver for (**SPCP<sub>sum</sub>**), which depends on a sequence of problems (**flip-SPCP<sub>sum</sub>**), converges slowly.

The ASALM performs reasonably well, which was unexpected since it was shown to be worse than NSA and PSPG in (Aybat et al., 2013; Aybat and Iyengar, 2013). The PSPG solver converges to the wrong answer, most likely due to a bad choice of the smoothing parameter  $\mu$ ; we tried choosing several different values other than the default but did not see improvement for this test (for other tests, not shown, tweaking  $\mu$  helped significantly). The NSA solver reaches moderate error quickly but stalls before finding a highly accurate solution.

### 5.2.2 SYNTHETIC TEST FROM AYBAT AND IYENGAR (2013)

We show some tests from the test setup of Aybat and Iyengar (2013) in the  $m = n = 1500$  case. The default setting of  $\lambda_{\text{sum}} = 1/\sqrt{\max(m, n)}$  was used, and then the NSA solver was run to high accuracy to obtain a reference solution  $(L^*, S^*)$ . From the knowledge of  $(L^*, S^*, \lambda_{\text{sum}})$ , one can generate  $\lambda_{\text{max}}, \tau_{\text{sum}}, \tau_{\text{max}}, \varepsilon$ , but not  $\lambda_S$  and  $\lambda_L$ , and hence we did not test the solvers for (**lag-SPCP**) in this experiment. The data were generated as  $A = L_0 + S_0 + Z_0$ , where  $L_0$  was sampled by multiplication of  $m \times r$  and  $r \times n$  normal Gaussian matrices,  $S_0$  had  $p$  randomly chosen entries uniformly distributed within  $[-100, 100]$ , and  $Z_0$  was white noise chosen to give a SNR of 45 dB. We show three tests that vary the rank from  $\{0.05, 0.1\} \cdot \min(m, n)$  and the sparsity ranging from

$p = \{0.05, 0.1\} \cdot mn$ . Unlike Aybat and Iyengar (2013), who report error in terms of a true noiseless signal  $(L_0, S_0)$ , we report the optimization error relative to  $(L^*, S^*)$ .

For the first test (with  $r = 75$  and  $p = 0.05 \cdot mn$ ),  $L^*$  had rank 786 and nuclear norm 111363.9;  $S^*$  had 75.49% of its elements nonzero and  $\ell_1$  norm 5720399.4, and  $\|L^* + S^* - A\|_F / \|A\|_F = 1.5 \cdot 10^{-4}$ . The other parameters were  $\varepsilon = 3.5068$ ,  $\lambda_{\text{sum}} = 0.0258$ ,  $\lambda_{\text{max}} = 0.0195$ ,  $\tau_{\text{sum}} = 2.5906 \cdot 10^5$  and  $\tau_{\text{max}} = 1.1136 \cdot 10^5$ . An interesting feature of this test is that while  $L_0$  is low-rank,  $L^*$  is nearly low-rank but with a small tail of significant singular values until number 786. We expect methods to converge quickly to low-accuracy, and then slow down as they try to find a highly-accurate larger rank solution.

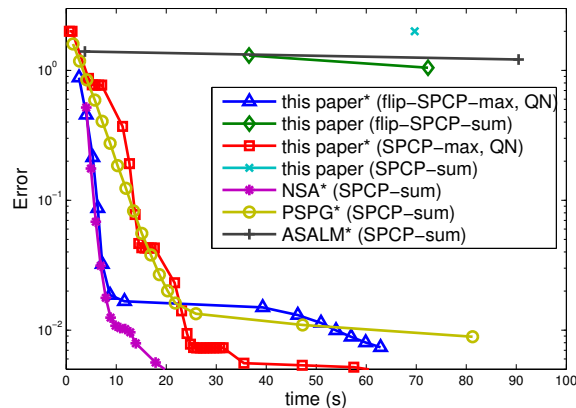


Figure 5: The  $1500 \times 1500$  synthetic noise test.

The results are shown in Fig. 5. Errors barely dip below 0.01 (for comparison, an error of 2 is achieved by setting  $L = S = 0$ ). The NSA and PSPG solvers do quite well. In contrast to the previous test, ASALM does poorly. Our methods for (**flip-SPCP<sub>sum</sub>**), and hence (**SPCP<sub>sum</sub>**), are not competitive, since they use dense SVDs. We imposed a time-limit of about one minute, so these methods only manage a single iteration or two. Our quasi-Newton method for (**flip-SPCP<sub>max</sub>**) does well initially, then takes a long time due to a long partial SVD computation. Interestingly, (**SPCP<sub>max</sub>**) does better than pure (**flip-SPCP<sub>max</sub>**). One possible explanation is that it chooses a fortuitous sequence of  $\tau$  values, for which the corresponding (**flip-SPCP<sub>max</sub>**) subproblems become increasingly hard, and therefore benefit from the warm-start of the solution of the easier previous problem. This is consistent with empirical observations regarding continuation techniques, see e.g., (Van den berg and Friedlander, 2008; Wright et al., 2009b).

Fig. 6 is the same test but with  $r = 150$  and  $p = 0.1 \cdot mn$ , and the conclusions are largely similar.

### 5.2.3 CLOUD REMOVAL

Figure 7 shows 15 images of size  $300 \times 300$  that come from the MODIS satellite<sup>7</sup>, after some transformations to turn images from different spectral bands into one grayscale images. Each image is a photo of the same rural location but at different points in time over the course of a few months. The background changes slowly and the variability is due to changes in vegetation, snow cover, and different reflectance. There are also outlying sources of error, mainly due to clouds (e.g., major

7. Publicly available at <http://ladsweb.nascom.nasa.gov/>

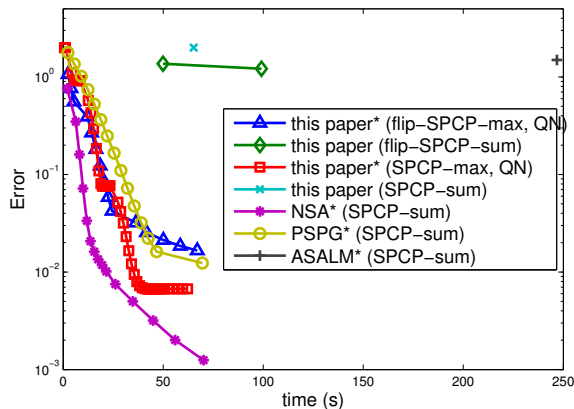


Figure 6: Second  $1500 \times 1500$  synthetic noise test.

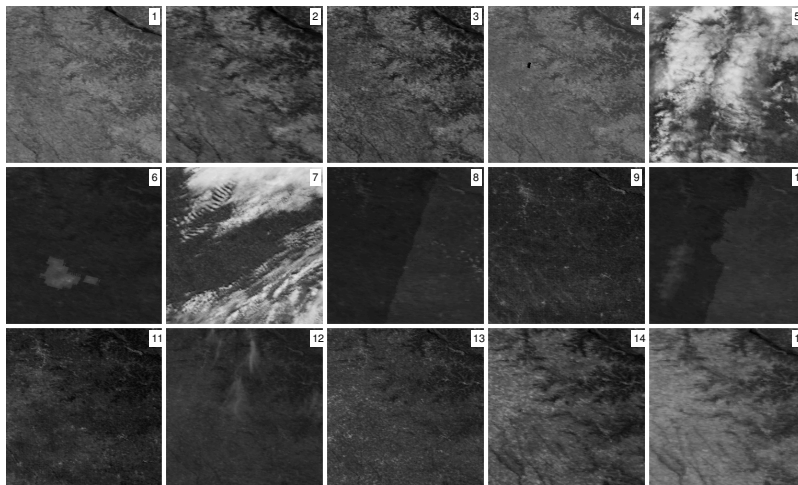


Figure 7: Satellite photos of the same location on different days.

clouds in frames 5 and 7, smaller clouds in frames 9, 11 and 12), as well as artifacts of the CCD camera on the satellite (frame 4 and 6) and issues stitching together photos of the same scene (the lines in frames 8 and 10).

There are many applications for clean satellite imagery, so removing the outlying error is of great practical importance. Because of slow changing background and sparse errors, we can model the problem using the robust PCA approach. We use the (flip-SPCP<sub>max</sub>) version due to its speed, and pick parameters  $(\lambda_{\max}, \tau_{\max})$  by using a Nelder-Mead simplex search. For an error metric to use in the parameter tuning, we remove frame 1 from the data set (call it  $y_1$ ) and set  $A$  to be frames 2–15. From this training data  $A$ , the algorithm generates  $L$  and  $S$ . Since  $L$  is a  $300^2 \times 14$  matrix, it has far from full column span. Thus our error is the distance of  $y_1$  from the span of  $L$ , i.e.,  $\|y_1 - \text{Proj}_{\text{span}(L)}(y_1)\|_2$ .

Our method takes about 11 iterations and 5 seconds, and uses a dense SVD instead of the randomized method due to the extremely high aspect ratio of the matrix: the matrix is  $15 \times 300^2$ , and the cost of a dense SVD is linear in the large dimension, so the computational burden is not

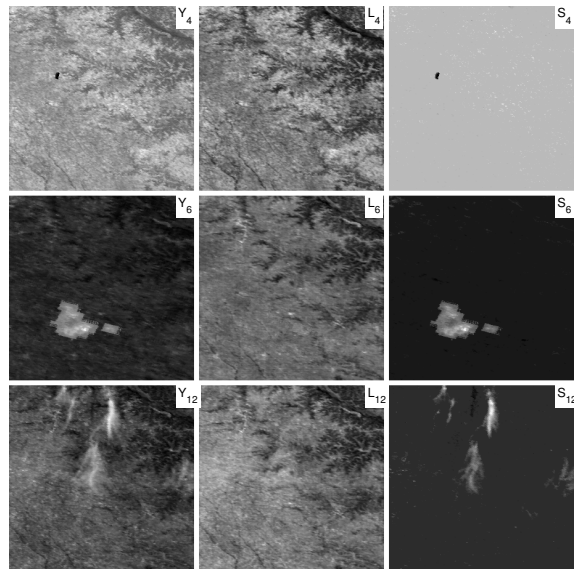


Figure 8: Showing frames 4, 5 and 12. Leftmost column is original data, middle column is low-rank term of the solution, and right column is sparse term of the solution. Data have been processed slightly to enhance contrast for viewing.

large. Some results of the obtained  $(L, S)$  outputs are in Fig. 8, where one can see that some of the anomalies in the original data frames  $A$  are picked up by the  $S$  term and removed from the  $L$  term. Frame 4 has what appears to be a camera pixel error; frame 6 has another artificial error (that is, caused by the camera and not the scene); and frame 12 has cloud cover.

#### 5.2.4 ANALYSIS OF BRAIN ACTIVITY IN THE ZEBRA FISH

Recent work by Ahrens et al. (2013) has produced video recordings of brain activity, in vivo, of zebra fish. These datasets are used to confirm scientific theories about the inner-working of the brain as well as to discover unexpected connections. Ultimately the goal is to discover causal, not just correlated, relationships. PCA on these datasets is one of the standard tools used by biologists in order to uncover correlations.

Using a public video of the dataset, we focus on a single 2D slice, sub-sampled spatially (and perhaps with video compression artifacts). We use ( $\text{SPCP}_{\max}$ ) as the RPCA technique, and therefore need to estimate  $\epsilon$  and  $\lambda_{\max}$ . To find  $\epsilon$ , we first take the SVD of the data matrix  $A$ . The corresponding singular values  $\sigma(A)$  are plotted in Fig. 9. This gives us an idea of the compressibility of the data. Keeping about 30 singular values explains over 99% of the data, so if we look for  $L$  with approximately rank 30, then, not including the sparse term  $S$  (which we expect to be very sparse), we should pick  $\epsilon \simeq \sqrt{\sum_{i=31}^{752} \sigma_i^2(A)}$ . This value works well in practice (see Fig. 10) and did not require cross-validation.

The  $\lambda_{\max}$  parameter is tuned by hand, but only takes 3 runs to find a reasonable value. This is much simpler than tuning  $\lambda_{\max}$  and  $\epsilon$  by hand simultaneously. Figure 10 shows the resulting top left singular vectors of  $A$  and of  $L$ , as well as their difference. We see that their difference is sparse, as

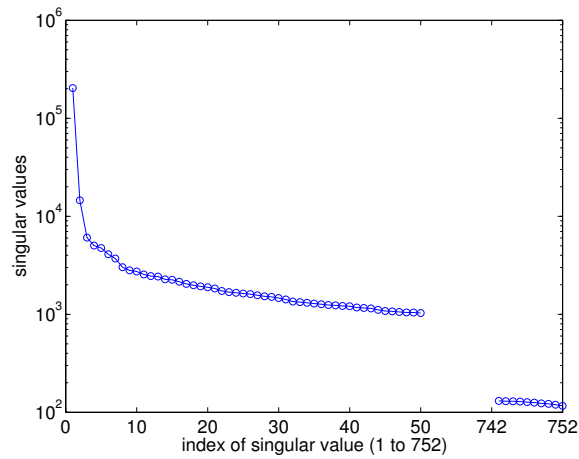
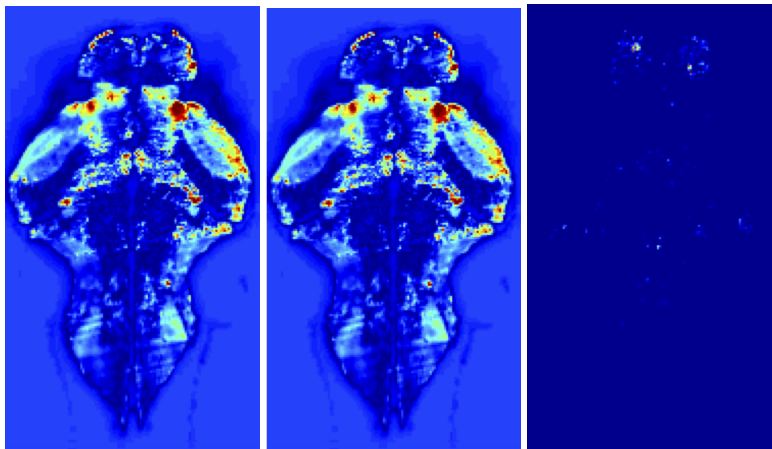


Figure 9: Decay of singular values of  $A$  for the zebra fish dataset. Singular values 51–742 are not shown.

expected. Since these are singular vectors, not just individual frames from the movie, these sparse differences are persistent over time, and perhaps meaningful. These unpredictable locations could be caused by sensor/microscope error, or they could mean that they come from a part of the brain that is not well correlated with general brain activity. Either way, it is useful to be able to separate out this effect.



(a) Top left singular vector of  $A$  (b) Top left singular vector of  $L$ . (c) Difference of (a) and (b).

Figure 10: Top left singular vector of  $A$  and of  $L$ , as well as their difference.

## 6. Conclusion

We have discussed both specific algorithms for the RPCA problem, and general algorithm frameworks (“TFOCS”, and “flipped” variational value-function approaches) that incorporate RPCA and variants. The custom RPCA algorithm works extremely well in practice, and the process of “flipping” the objective has been studied rigorously, but the inner “quasi-Newton” algorithm lacks a rigorous convergence theory. The general algorithm TFOCS, as well as similar proposals such as the PDHG algorithm, have more established theory but lack practical guidance on setting parameters, and are in practice slower than the special purpose algorithms. An obvious goal of future work is to either improve the analysis of these algorithms (for example, this may give insight into parameter selection), or derive new algorithms that inherit all the advantages.

The running theme of this work has been the benefits of solving variants of RPCA, in particular (**flip-SPCP<sub>sum</sub>**) and the new variants (**SPCP<sub>max</sub>**) and (**flip-SPCP<sub>max</sub>**). These versions sometimes allow a good estimate of  $\tau$  (or  $\varepsilon$  for (**SPCP<sub>max</sub>**)), thus reducing the parameter selection of the model to the single scalar  $\lambda_{\text{sum}}$  or  $\lambda_{\text{max}}$ . Our theory allows for different regularizers and data fidelity terms; using these in practice is interesting future work.

## References

- M. B. Ahrens, M. B. Orger, D. N. Robson, J. M. Li, and P. J. Keller. Whole-brain functional imaging at cellular resolution using light-sheet microscopy. *Nature Methods*, 10(413–420), 2013.
- A. Aravkin, S. Becker, V. Cevher, and P. Olsen. A variational approach to stable principal component pursuit. In *Uncertainty in Artificial Intelligence*, Quebec City, 2014a.
- A. Y. Aravkin, J. V. Burke, and M. P. Friedlander. Variational properties of value functions. *SIAM J. Opt.*, 23(3):1689–1717, 2013.
- A.Y. Aravkin, R. Kumar, H. Mansour, B. Recht, and F.J. Herrmann. Fast methods for denoising matrix completion formulations, with applications to robust seismic data interpolation. *SIAM Journal on Scientific Computing*, 36(5):S237–S266, 2014b.
- A.Y. Aravkin, R. Kumar, H. Mansour, B. Recht, and F.J. Herrmann. Fast methods for denoising matrix completion formulations, with applications to robust seismic data interpolation. *SIAM Journal on Scientific Computing*, 36(5):S237–S266, 2014c.
- A.Y. Aravkin, J.V. Burke, D. Drusvyatskiy, M.P. Friedlander, and S. Roy. Level-set methods for convex optimization. *arXiv preprint arXiv:1602.01506*, 2016.
- N. Aybat, D. Goldfarb, and S. Ma. Efficient algorithms for robust and stable principal component pursuit. *Computational Optimization and Applications*, accepted, 2013.
- N. S. Aybat and G. Iyengar. A fast first-order method for stable principal component pursuit. <http://arxiv.org/abs/1309.6553>, 2013.
- H.H. Bauschke and P. Combettes. *Convex analysis and monotone operators theory in Hilbert spaces*. Springer-Verlag, 2011.

- A. Beck and M. Teboulle. A Fast Iterative Shrinkage-Thresholding Algorithm for Linear Inverse Problems. *SIAM J. Imaging Sciences*, 2(1):183–202, January 2009a.
- A. Beck and M. Teboulle. A fast iterative shrinkage-thresholding algorithm for linear inverse problems. *SIAM J. Imaging Sci.*, 2(1):183–202, 2009b. ISSN 1936-4954. doi: 10.1137/080716542. URL <http://dx.doi.org/10.1137/080716542>.
- A. Beck and M. Teboulle. A fast dual proximal gradient algorithm for convex minimization and applications. *Operations Research Letters*, 42(1):1–6, 2014. ISSN 0167-6377. doi: <http://dx.doi.org/10.1016/j.orl.2013.10.007>. URL <http://www.sciencedirect.com/science/article/pii/S0167637713001454>.
- S. Becker. *Practical Compressed Sensing: modern data acquisition and signal processing*. PhD thesis, California Institute of Technology, Pasadena, CA, 2011.
- S. Becker and E. Candès. Singular value thresholding toolbox, 2008. Available from <http://svt.stanford.edu/>.
- S. Becker and P. L. Combettes. An algorithm for splitting parallel sums of linearly composed monotone operators, with applications to signal recovery. *J. Nonlinear and Convex Analysis*, 15(1):137–159, 2014.
- S. Becker, E. J. Candès, and M. Grant. Templates for convex cone problems with applications to sparse signal recovery. *Math. Prog. Comp.*, 3(3):165–218, 2011.
- D. P. Bertsekas. Necessary and sufficient conditions for a penalty method to be exact. *Math. Program.*, 9:87–99, 1975.
- D. P. Bertsekas, A. Nedić, and A. E. Ozdaglar. *Convex Analysis and Optimization*. Athena Scientific, 2003.
- R. I. Boş and E. R. Csetnek. Forward-backward and Tsengs type penalty schemes for monotone inclusion problems. *Set-Valued and Variational Analysis*, 22(2):313–331, 2014. ISSN 1877-0533. doi: 10.1007/s11228-014-0274-7. URL <http://dx.doi.org/10.1007/s11228-014-0274-7>.
- R. I. Boş, E. R. Csetnek, and A. Heinrich. A primal-dual splitting algorithm for finding zeros of sums of maximal monotone operators. *SIAM Journal on Optimization*, 23(4):2011–2036, 2013a. doi: 10.1137/12088255X. URL <http://dx.doi.org/10.1137/12088255X>.
- R. I. Boş, E. R. Csetnek, and E. Nagy. Solving systems of monotone inclusions via primal-dual splitting techniques. *Taiwanese Journal of Mathematics*, 17(6):pp–1983, 2013b.
- R. I. Boş, E. R. Csetnek, A. Heinrich, and C. Hendrich. On the convergence rate improvement of a primal-dual splitting algorithm for solving monotone inclusion problems. *Mathematical Programming*, 150(2):251–279, 2015. ISSN 0025-5610. doi: 10.1007/s10107-014-0766-0. URL <http://dx.doi.org/10.1007/s10107-014-0766-0>.

- T. Bouwmans and E. H. Zahzah. Robust PCA via principal component pursuit: A review for a comparative evaluation in video surveillance. *Computer Vision and Image Understanding*, 122(0): 22–34, 2014. ISSN 1077-3142. doi: <http://dx.doi.org/10.1016/j.cviu.2013.11.009>. URL <http://www.sciencedirect.com/science/article/pii/S1077314213002294>.
- L. M. Briceo-Arias and P. L. Combettes. A monotone+skew splitting model for composite monotone inclusions in duality. *SIAM J. Optim.*, 21(4):1230–1250, 2011.
- P. Brucker. An  $O(n)$  algorithm for quadratic knapsack problems. *Operations Res. Lett.*, 3(3):163–166, 1984. doi: 10.1016/0167-6377(84)90010-5.
- J. J. Bruer, J. A. Tropp, V. Cevher, and S. Becker. Time–data tradeoffs by aggressive smoothing. In *Advances in Neural Information Processing Systems*, pages 1664–1672, 2014.
- J. Burke and M. Qian. A variable metric proximal point algorithm for monotone operators. *SIAM J. Control Opt.*, 37(2):353–375, 1997.
- J.-F. Cai, E. J. Candès, and Z. Shen. A singular value thresholding algorithm for matrix completion. *SIAM J. Optim.*, 20:1956–1982, 2010.
- E. J. Candès and Y. Plan. Matrix completion with noise. *Proceedings of the IEEE*, 98(6):925–936, 2010.
- E. J. Candès, X. Li, Y. Ma, and J. Wright. Robust principal component analysis? *J. Assoc. Comput. Mach.*, 58(3):1–37, May 2011a.
- E.J. Candès, X. Li, Y. Ma, and J. Wright. Robust principal component analysis? *J. ACM*, 58(3):11:1–11:37, June 2011b. ISSN 0004-5411. doi: 10.1145/1970392.1970395. URL <http://doi.acm.org/10.1145/1970392.1970395>.
- V. Cevher, S. Becker, and M. Schmidt. Convex optimization for big data: Scalable, randomized, and parallel algorithms for big data analytics. *IEEE Sig. Proc. Mag.*, 31(5):32–43, 2014.
- A. Chambolle and C. Dossal. On the convergence of the iterates of “FISTA”. Technical Report hal-01060130, HAL, 2014. <https://hal.inria.fr/hal-01060130v3>.
- A. Chambolle and T. Pock. A first-order primal-dual algorithm for convex problems with applications to imaging. *J. Math. Imaging Vision*, 40(1):120–145, 2010.
- V. Chandrasekaran, S. Sanghavi, P. A. Parrilo, and A. S. Willsky. Sparse and low-rank matrix decompositions. In *SYSID 2009*, Saint-Malo, France, July 2009.
- V. Chandrasekaran, P. A. Parrilo, and A. S. Willsky. Latent variable graphical model selection via convex optimization. *Ann. Stat.*, 40(4):1935–2357, 2012.
- C. Chen, B. He, Y. Ye, and X. Yuan. The direct extension of admm for multi-block convex minimization problems is not necessarily convergent. *Optimization Online*, 2013.
- P. G. Ciarlet. *Introduction to numerical linear algebra and optimisation*. Cambridge University Press, 1989.

- P. L. Combettes. Systems of structured monotone inclusions: duality, algorithms, and applications. *SIAM J. Optimization*, 23(4):2420–2447, 2013.
- P. L. Combettes and J.-C. Pesquet. A DouglasRachford Splitting Approach to Nonsmooth Convex Variational Signal Recovery. *IEEE J. Sel. Topics Sig. Processing*, 1(4):564–574, December 2007.
- P. L. Combettes and J.-C. Pesquet. Proximal splitting methods in signal processing. In H. H. Bauschke, R. S. Burachik, P. L. Combettes, V. Elser, D. R. Luke, and H. Wolkowicz, editors, *Fixed-Point Algorithms for Inverse Problems in Science and Engineering*, pages 185–212. Springer-Verlag, New York, 2011.
- P. L. Combettes and J.-C. Pesquet. Primal-dual splitting algorithm for solving inclusions with mixtures of composite, Lipschitzian, and parallel-sum type monotone operators. *Set-Valued and Variational Analysis*, 20(2):307–330, 2012.
- P. L. Combettes and V. R. Wajs. Signal recovery by proximal forward-backward splitting. *Multiscale Model. Simul.*, 4(4):1168–1200 (electronic), 2005. ISSN 1540-3459. doi: 10.1137/050626090. URL <http://dx.doi.org/10.1137/050626090>.
- P. L. Combettes, D. Dũng, and B. C. Vũ. Dualization of signal recovery problems. *Set-Valued and Variational Analysis*, 18:373–404, 2010. ISSN 1877-0533.
- L. Condat. A primal-dual splitting method for convex optimization involving Lipschitzian, proximal and linear composite terms. *J. Optim. Theory Appl.*, pages 460–479, 2013.
- O. Devolder, F. Glineur, and Y. Nesterov. First-order methods of smooth convex optimization with inexact oracle. *Math. Prog.* submitted, 2011.
- O. Devolder, F. Glineur, and Y. Nesterov. Double smoothing technique for large-scale linearly constrained convex optimization. *SIAM Journal on Optimization*, 22(2):702–727, 2012. doi: 10.1137/110826102. URL <http://dx.doi.org/10.1137/110826102>.
- J. Duchi, S. Shalev-Shwartz, Y. Singer, and T. Chandra. Efficient projections onto the  $l_1$ -ball for learning in high dimensions. In *Intl. Conf. Machine Learning (ICML)*, pages 272–279, New York, July 2008. ACM Press.
- E. Esser, X. Zhang, and T. Chan. A general framework for a class of first order primal-dual algorithms for tv minimization. Technical Report 09-67, UCLA, Center for Applied Math, 2009.
- M. P. Friedlander and P. Tseng. Exact regularization of convex programs. *SIAM J. Optim.*, 18(4): 1326–1350, 2007. doi: 10.1137/060675320. URL <http://link.aip.org/link/?SJE/18/1326/1>.
- A. Ganesh, Z. Lin, J. Wright, L. Wu, M. Chen, and Y. Ma. Fast algorithms for recovering a corrupted low-rank matrix. In *Computational Advances in Multi-Sensor Adaptive Processing (CAMSAP)*, pages 213–215, Aruba, Dec. 2009.
- D. Goldfarb, S. Ma, and K. Scheinberg. Fast alternating linearization methods for minimizing the sum of two convex functions. *Math. Prog. (Series A)*, 141(1–2):349–382, 2013.

- T. Goldstein, E. Esser, and R. Baraniuk. Adaptive primal-dual hybrid gradient methods for saddle-point problems. Technical report, 2013. <http://arxiv.org/abs/1305.0546>.
- N. Halko, P.-G. Martinsson, and J. A. Tropp. Finding structure with randomness: Probabilistic algorithms for constructing approximate matrix decompositions. *SIAM review*, 53(2):217–288, 2011.
- B.S. He and X. M. Yuan. Convergence analysis of primal-dual algorithms for a saddle-point problem: from contraction perspective. *SIAM J. Imaging Sci.*, pages 119–149, 2012a.
- B.S. He and X.M. Yuan. On the  $o(1/n)$  convergence rate of the Douglas-Rachford alternating direction method. *SIAM J. Numer. Anal.*, 50(700–709), 2012b.
- P. J. Huber. *Robust Statistics*. John Wiley and Sons, 2 edition, 2004.
- N. Komodakis and J.-C. Pesquet. Playing with duality: An overview of recent primal-dual approaches for solving large-scale optimization problems. *IEEE Sig. Pro. Magazine*, to appear, May 2015. <http://arxiv.org/abs/1406.5429v2>.
- M. Lai and W. Yin. Augmented  $\ell_1$  and nuclear-norm models with a globally linearly convergent algorithm. *SIAM J. Imaging Sci.*, 6(2):1059–1091, 2013.
- J. Lee, B. Recht, R. Salakhutdinov, N. Srebro, and J.A. Tropp. Practical large-scale optimization for max-norm regularization. In *Neural Information Processing Systems (NIPS)*, Vancouver, 2010.
- X. X. Li, L. L. Mo, X. M. Yuan, and J. Z. Zhang. Linearized alternating direction method of multipliers for sparse group and fused LASSO models. *Comput. Statis. Data Anal.*, 79:203–221, 2014.
- Z. Lin, M. Chen, and Y. Ma. The augmented Lagrange multiplier method for exact recovery of corrupted low-rank matrices. *arXiv preprint arXiv:1009.5055*, 2010.
- Y.-J. Liu, D. Sun, and K.-C. Toh. An implementable proximal point algorithmic framework for nuclear norm minimization. *Mathematical Programming*, 2011.
- F. Bach M. Schmidt, N. Le Roux. Convergence rates of inexact proximal-gradient methods for convex optimization. In *NIPS*, 2011.
- F. Malgouyres and T. Zeng. A predual proximal point algorithm solving a non negative basis pursuit denoising model. *Int. J. Comp. Vision*, 83(3):294–311, July 2009.
- O. L. Mangasarian and R. R. Meyer. Nonlinear perturbation of linear programs. *SIAM J. Control Optim.*, 17:745–752, 1979.
- J.-J. Moreau. Proximité et dualité dans un espace hilbertien. *Bull. Soc. Math. France*, 93:273–299, 1965.
- I. Necoara and J. A. K. Suykens. Application of a smoothing technique to decomposition in convex optimization. *IEEE Trans. Auto. Control*, 53(11):2674–2679, 2008.

- Y. Nesterov. A method of solving a convex programming problem with convergence rate  $\mathcal{O}(1/k^2)$ , in soviet mathematics doklady. *Soviet Mathematics Doklady*, 27, 1983.
- Y. Nesterov. *Introductory lectures on convex optimization: a basic course*, volume 87 of *Applied Optimization*. Kluwer Academic Publishers, 2004.
- Y. Nesterov. Smooth minimization of non-smooth functions. *Math. Program., Ser. A*, 103:127–152, 2005.
- J. Nocedal and S. Wright. *Numerical Optimization*. Springer, 2 edition, 2006.
- Y. Peng, A. Ganesh, J. Wright, W. Xu, and Y. Ma. RASL: Robust alignment by sparse and low-rank decomposition for linearly correlated images. *IEEE Trans. Pattern Analysis and Machine Intelligence*, 34(11):2233–2246, 2012. ISSN 0162-8828. doi: <http://doi.ieeecomputersociety.org/10.1109/TPAMI.2011.282>.
- T. Pock and A. Chambolle. Diagonal preconditioning for first order primal-dual algorithms in convex optimization. In *Computer Vision (ICCV), 2011 IEEE International Conference on*, pages 1762–1769, Nov 2011. doi: 10.1109/ICCV.2011.6126441.
- B. T. Poljak and N. V. Tretjakov. An iterative method for linear programming and its economic interpretation. *Matecon*, 10:81–100, 1974.
- X. Ren and Z. Lin. Linearized alternating direction method with adaptive penalty and warm starts for fast solving transform invariant low-rank textures. *Int. J. Comput. Vis.*, 104:1–14, 2013.
- R. T. Rockafellar. *Convex analysis*. Princeton Mathematical Series, No. 28. Princeton University Press, Princeton, N.J., 1970a.
- R. T. Rockafellar. Monotone operators and the proximal point algorithm. *SIAM Journal on Control and Optimization*, 14:877–898, 1976.
- R. Tyrrell Rockafellar. *Convex Analysis*. Princeton Landmarks in Mathematics. Princeton University Press, 1970b.
- R. Tyrrell Rockafellar and Roger J-B. Wets. *Variational Analysis*, volume 317 of *A Series of Comprehensive Studies in Mathematics*. Springer, 1998.
- M. Schmidt, E. van den Berg, M. Friedlander, and K. Murphy. Optimizing costly functions with simple constraints: A limited-memory projected quasi-Newton algorithm. In *AISTATS*, 2009.
- Y. Shen, Z. Wen, and Y. Zhang. Augmented Lagrangian alternating direction method for matrix separation based on low-rank factorization. *Optimization Methods and Software*, 29(2):239–263, March 2014.
- Z. Shi, J. Han, T. Zheng, and J. Li. Guarantees of augmented trace norm models in tensor recovery. In *Int. Joint Conf. Artificial Intell.*, pages 1670–1676, 2013.
- M. Tao and X. Yuan. Recovering low-rank and sparse components of matrices from incomplete and noisy observations. *SIAM J. Optimization*, 21:57–81, 2011.

- Q. Tran-Dinh and V. Cevher. Constrained convex minimization via model-based excessive gap. In Z. Ghahramani, M. Welling, C. Cortes, N.D. Lawrence, and K.Q. Weinberger, editors, *Advances in Neural Information Processing Systems 27*, pages 721–729. Curran Associates, Inc., 2014. URL <http://papers.nips.cc/paper/5494-constrained-convex-minimization-via-model-based-excessive-gap.pdf>.
- E. van den Berg and M. P. Friedlander. Probing the Pareto frontier for basis pursuit solutions. *SIAM J. Sci. Comput.*, 31(2):890–912, 2008.
- E. Van den berg and M. P. Friedlander. Probing the Pareto frontier for basis pursuit solutions. *SIAM J. Sci. Computing*, 31(2):890–912, 2008. software: <http://www.cs.ubc.ca/~mpf/spgl1/>.
- E. van den Berg and M. P. Friedlander. Sparse optimization with least-squares constraints. *SIAM J. Optimization*, 21(4):1201–1229, 2011.
- S. Villa, S. Salzo, L. Baldassare, and A. Verri. Accelerated and inexact forward-backward algorithms. *SIAM J. Optimization*, 23(3):1607–1633, 2013. doi: 10.1137/110844805.
- B. C. Vũ. A splitting algorithm for dual monotone inclusions involving cocoercive operators. *Adv. Comput. Math*, 38(3):667–681, 2013.
- X. Wang and X. M. Yuan. The linearized alternating direction method of multipliers for Dantzig selector. *SIAM J. Sci. Comput.*, 34:2782–2811, 2012.
- J. Wright, A. Ganesh, S. Rao, and Y. Ma. Robust principal component analysis: Exact recovery of corrupted low-rank matrices by convex optimization. In *Neural Information Processing Systems (NIPS)*, 2009a.
- S. J. Wright, R. D. Nowak, and M. A. T. Figueiredo. Sparse reconstruction by separable approximation. *IEEE Trans. Sig. Processing*, 57(7):2479–2493, July 2009b.
- J. Yang and Y. Zhang. Alternating direction algorithms for  $l_1$ -problems in compressive sensing. *SIAM J. Sci. Comput.*, 33(1–2):250–278, 2011.
- J. F. Yang and X. M. Yuan. Linearized augmented Lagrangian and alternating direction methods for nuclear norm minimization. *Math. Comput.*, 82:301–329, 2013.
- W. Yin. Analysis and generalizations of the linearized Bregman method. *SIAM J. Imaging Sci.*, 3(4):856–877, 2010. doi: 10.1137/090760350. URL <http://link.aip.org/link/?SII/3/856/1>.
- Q. You, Q. Wan, and Y. Liu. A short note on strongly convex programming for exact matrix completion and robust principal component analysis. *Inverse Problems and Imaging*, 7(1):305–306, 2013.
- J. Zhang, J.-F. Cai, L. Cheng, and J. Zhu. Strongly convex programming for exact matrix completion and robust principal component analysis. *Inverse Problems and Imaging*, 6(2):357–372, 2012.
- X. Q. Zhang, M. Burger, and S. Osher. A unified primal-dual algorithm framework based on Bregman iteration. *J. Sci. Comput.*, 46:20–46, 2010.

- Z. Zhang, X. Liang, A. Ganesh, and Y. Ma. TILT: Transform invariant low-rank textures. In R. Kimmel, R. Klette, and A. Sugimoto, editors, *Computer Vision – ACCV 2010*, volume 6494 of *Lecture Notes in Computer Science*, pages 314–328. Springer, 2011.
- X.-Y. Zhao, D. Sun, and K.-C. Toh. A Newton-CG augmented Lagrangian method for semidefinite programming. *SIAM Journal on Optimization*, 20(4):1737–1765, 2010. doi: 10.1137/080718206. URL <http://dx.doi.org/10.1137/080718206>.